SIMULATION OF FLUIDIZED BED DRYER

A DISSERTATION

Submitted in partial fulfillment of the requirements for the award of the degree
of
MASTER OF TECHNOLOGY
in
CHEMICAL ENGINEERING
(with specialization in Computer Aided Process Plant Design)

By

SOMASEKHAR BADUGU

DEPARTMENT OF CHEMICAL ENGINEERING
INDIAN INSTITUTE OF TECHNOLOGY ROORKEE
ROORKEE - 247 667 (INDIA)
JUNE, 2007

CANDIDATE'S DECLARATION

I hereby declare that the work, presented in this dissertation report entitled **"Simulation of Fluidized bed Dryer"** in partial fulfillment of the requirement for the award of the degree **Master of Technology** in **Chemical Engineering** with specialization in **Computer Aided Process Plant Design (CAPPD)**, and submitted in the **Department of Chemical Engineering** of **Indian Institute of Technology Roorkee**, Roorkee, under supervision of **Dr.V.K. AGARWAL**, Associate Professor, Department of Chemical Engineering, Indian Institute of Technology Roorkee, Roorkee.

I have not submitted the matter, embodied in this dissertation report for the award of any other degree.

Place: Roorkee,
Date: 26 June, 2007

B. Somasekhar
(SOMA SEKHAR BADUGU)

CERTIFICATE

This is to certify that the above statement made by the candidate is correct to the best of my knowledge and belief.

26.6.07
DR. V.K. AGARWAL
Associate Professor,
Department of Chemical Engineering,
Indian Institute of Technology, Roorkee,
Roorkee – 247667.

ACKNOWLEDGEMENT

I take the opportunity to pay my regards and a deep sense of gratitude to my guide **Dr.V.K.Agarwal**, Associate Professor, Department of Chemical Engineering, Indian Institute of Technology Roorkee, Roorkee for his valuable guidance, keen cooperation suggestions and constant encouragement during all stages of preparation of this dissertation report. It was in deed a very pleasant, educative and motivating experience for me while working under his kind guidance.

Most sincere thanks are due to Dr. Shri Chand, Professor and head of the Department of Chemical Engineering, Indian Institute of Technology Roorkee, Roorkee for providing all facilities and help during this dissertation.

I would like to thank all my fellow students, for their valuable suggestions in the work.

Above all, I would like to acknowledge that the greatest role has been of my parents who have helped me to cultivate the system of values and instincts that shall always enlighten my path all these living years.

Thanks are due to CAD Centre Facilities

Place: Roorkee;

Dated : june 2007. **(SOMA SEKHAR BADUGU)**

ABSTRACT

This thesis describes the simulation of fluidized bed dryer. Basically it deals with the development of a mathematical model of fluidized bed dryer based on two phase theory of fluidization. Further the mathematical model has been validated with the data of "Lai & Yiming Chen" in the end the effect of operating parameters on the performance characteristics has been investigated. The operating parameters include particle inlet moisture content of the drying gas, temperature of the drying particle, diameter of the drying particle, density of the drying particle, residence time of the drying particle and superficial air velocity of the drying gas.

A fluidized bed includes two phases one is the emulsion phase and the other is the bubble phase. Solid particles in the emulsion phase are lumped and in the bubble is assumed plug flow regime, whereas emulsion phase is considered to be in mixed flow regime. Bubble size is one of the most important parameter in the design and simulation of fluidized bed dryer. A correlation of bubble size in fluidized bed dryer is incorporated.

The developed mathematical model has been solved by Matlab 7.0. numerical simulation based on the model was done and the model is tested against the data of "Lai and Yiming Chen and found in good agreement with the maximum deviation of 3%.

The parametric effects on the output variables namely "the moisure content of the outlet solid and the temperature of the outlet solid" has been investigated on the performance of the dryer.

CONTENTS

	Page No.
CANDIDATE'S DECLARATION	I
ACKNOWLEDGEMENT	II
ABSTRACT	III
CONTENTS	IV
LIST OF TABLES	VI
LIST OF FIGURES	VII
NOMENCLATURE	VIII
CHAPTER 1 INTRODUCTION	1
1.1 FLUIDIZED BED DRYER	2
1.2 VIBRATED FLUID BED	2
1.3 FLUID -BED GRANULATION	3
1.4 SPOUTED BED DRYER	3
1.5 MECHANICALLY AGITATED FLUID -BED DRYER	3
1.6 CENTRIFUGAL FLUID-BED DRYERS	3
1.7 FLUIDIZED SPRAY DRYER	3
1.8 ADVANTAGES OF FLUIDIZED BEDS	4
1.9 DISADVANTAGES OF FLUIDIZED BEDS	5
1.10 OBJECTIVE OF OUR PRESENT STUDY	5
CHAPTER 2 LITERATURE REVIEW	6
CHAPTER 3 MATHEMATICAL MODELLING	20
3.1 MODEL DEVELOPMENT	20
3.2 ASSUMPTIONS	21
3.3 MASS CONSERVATION EQUATIONS	21
3.4 ENERGY CONSERVATION EQUATIONS	22
3.5 CORRELATIONS	23

CHAPTER 4 SOLUTION OF THE NUMERICAL MODEL 26
CHAPTER 5 RESULTS AND DISCUSSIONS 29
CHAPTER 6.0 RECOMMENDATIONS & CONCLUSION 45
6.1 CONCLUSION 45
6.2 RECOMMENDATIONS 45
REFERENCES 46
APPENDIX-I 48

LIST OF TABLES

Tab No.	*Title*	*Page No.*
2.1.	Summary of correlations for bubble diameter in fluidized beds	7

LIST OF FIGURES

Fig. No.	*Caption*	*Page No.*
1.1.	Fluidized-bed Dryer	2
3.1.	Schematic Diagram of Continuous Drying in the Fluidized bed	20
4.1.	Algorithm of solution	28
5.1.	Comparison of the Moisture Content of the outlet Solid Particle as a function of Time	31
5.2.	Comparison of the Temperature of the outlet Solid Particle as a function of time	32
5.3.	Variation of Moisture Content of the Dried Product as a function of time and initial Moisture content	34
5.4.	Variation of Moisture Content of the Dried Product as a function of time and Superficial air Velocity	36
5.5.	Variation in the Temperature of the Dried Product as a function of time and Superficial air velocity	37
5.6.	Variation of Moisture Content of the Dried Product as a function of time and Residence Time of the Solid particle	39
5.7.	Variation in Temperature of the Dried Product as a function of time and Residence time of the Solid Particle	40
5.8.	Variation in Moisture Content of the Dried Product as a function of time and initial Temperature of the Solid particle	42
5.9.	Variation of Moisture Content of the Dried Product as a function of time and Particle Diameter	43
5.10.	Variation of Moisture Content of the Dried Product as a function of Time and Solid Density	44

NOMENCLATURE

Variable	Description	Units
A_t	Cross-sectional area of the bed	m^2
A_b	Cross-sectional area of the bubble phase	m^2
a_w	Specific heat-transfer surface of the dryer wall	m^{-1}
c_g	Specific heat of drying gas	$kJ\ kg^{-1}\ {}^0C^{-1}$
c_p	Specific heat of particles (dry basis)	$kJkg^{-1}\ {}^0C^{-1}$
c_w	Specific heat of water (liquid state)	$kJkg^{-1}\ {}^0C^{-1}$
c_{wv}	Specific heat of water vapour	$kJkg^{-1}\ {}^0C^{-1}$
D_c	Diameter of the bed column	m
D_g	Molecular diffusion coefficient of the drying gas	$m^2\ s^{-1}$
D_{geff}	Effective diffusion coefficient of the drying gas	$m^2\ s^{-1}$
d_b	Effective bubble diameter	m
d_p	Particle diameter	m
g	Gravitational acceleration	$m\ s^{-2}$
H_f	Expanded bed height	m
H_{mf}	Bed height at mininum fluidizing conditions	m
$(H_{bc})_b$	Volumetric heat-transfer coefficient between the bubble & cloud-wake regions based on the volume of bubbles	$J\ s^{-1}\ m^{-3}\ {}^0C^{-1}$
$(H_{be})_b$	Volumetric heat-transfer coefficient between the bubble and emulsion phases based on the volume of bubbles	$J\ s^{-1}\ m^{-3}\ {}^0C^{-1}$
$(H_{ce})_b$	Volumetric heat-transfer coefficient between the cloud-wake region and the emulsion phase based on the volume	$J\ s^{-1}\ m^{-3}\ {}^0C^{-1}$
h_p	Heat-transfer coefficient between the drying gas and solids	$Js^{-1}m^{-2}\ {}^0C^{-1}$

h_w	Heat-transfer coefficient between the drying gas and the dryer wall	$Js^{-1}\,m^{-2}\,{}^0C^{-1}$
i_0	Enthalpy of inlet gas (dry basis)	$kJ\,kg^{-1}$
i_b	Enthalpy of gas bubbles (dry basis)	$kJ\,kg^{-1}$
i_e	Enthalpy of the emulsion gas (dry basis)	$kJ\,kg^{-1}$
i_{ws}	Enthalpy of water vapour on the surface of a particle	$kJ\,kg^{-1}$
$\bar{i}_{ws}$	Average enthalpy of water vapour on the surface of particles	$kJ\,kg^{-1}$
i_{we}	Enthalpy of water vapour contained in the emulsion gas	$kJ\,kg^{-1}$
i_p	Enthalpy of a particle (wet basis)	$kJ\,kg^{-1}$
j_p	Colburn factor	---
$(K_{be})_b$	Coefficient of gas interchange between the bubble and cloud- wake regions based on the volume of bubbles	s^{-1}
$(K_{be})_b$	Coefficient of gas interchange between the bubble and Emulsion phases based on the volume of bubbles	s^{-1}
$(K_{ce})_b$	Coefficient of gas interchange between the cloud-wake region and the emulsion phase based on the volume of bubbles	s^{-1}
k_g	Thermal conductivity of the drying gas	$Jm^{-1}\,{}^0C^{-1}$
Le	Lewis number	---
Nu	Nusselt number	---
Pr	Pranetl number	---
P_w	Pressure of saturated water vapour,	mm Hg
q_s	Conductive heat flux inside a particle,	$J\,s^{-1}\,m^{-2}$
Re_p	Particle Reynolds number	---
S_w	Heat-transfer surface area of the dryer wall	m^2
T_0	Temperature of the inlet gas	${}^0C$
T_b	Temperature of gas bubbles	${}^0C$
$\bar{T}_b$	Bed-height average temperature of gas bubbles	${}^0C$
T_e	Temperature of the emulsion gas	${}^0C$

T_{out}	Temperature of the outlet gas	^0C
T_p	Temperature of a particle	^0C
$\overline{T}_p$	Average temperature of particles	^0C
T_{p0}	Temperature of inlet particles	^0C
T_{ref}	Reference-state temperature	^0C
T_w	Dryer-wall temperature	^0C
t_s	Time,	s
$\overline{t}_s$	Mean residence time of particles in the dryer	s
U_0	Superficial gas velocity (measured on an empty bed basis) through a bed of solids	m s^{-1}
U_b	Superficial gas velocity in the bubble phase, based on totalcross-sectional area of the bed	m s^{-1}
U_{br}	Linear velocity of a single bubble	m s^{-1}
U_{mf}	Superticial gas velocity at minimum fluidizing conditions	m s^{-1}
V_t	Volume of the bed	m^3
x_0	Moisture content of inlet gas (dry basis)	---
x_b	Moisture content of gas bubbles (dry basis)	---
$\overline{x}_b$	Bed-height average moisture content of gas bubbles (dry basis)	---
x_e	Moisture content of the emulsion gas (dry basis),	---
x_{out}	Moisture content of outlet gas (dry basis)	---
x_p	Moisture content of a particle (dry basis)	---
$\overline{x}_p$	Average moisture content of particles (dry basis),	---
x_p^*	Moisture content of the drying gas on the surface of	---
	a particle (dry basis)	---
$\overline{x}_p^*$	Average moisture content of the drying gas on the	---
	surface of a particle (dry basis)	---
x_{p0}	Moisture content of inlet particles (dry basis)	---
x_{pc}	Critical moisture content of a particle (dry basis)	---

z	Elevation,	m
Greek symbols		
γ_0	Heat of vaporization,	kJ kg^{-1}
δ_b	Fraction of the fluidized bed consisting of bubbles	--
ε_e	Void fraction in the emulsion phase	--
ε_{mf}	Void fraction at minimum fluidizing conditions	--
μ_g	Viscosity of gas	kgm^{-1} s^{-1}
ρ_g	Density of gas	kg m^{-3}
ρ_s	Density of dry solids	kg m^{-3}
ρ_w	Density of water	kg m^{-3}
ρ_{ws}	Density of wet solids	kg m^{-3}
σ	Evaporation coefficient	kg m^{-2} s^{-1}
ϕ	Sphericity of a particle	--

INTRODUCTION

A myriad of chemical industries use drying as a major process step. The cost of drying is reported to consume 60% of the total energy in manufacturing processes. Pharmaceutical, food, biological, and petrochemical processes all use drying technology. Due to the high gas-solid contact, low maintenance, and uniform product delivery fluidized bed drying (FBD) is the superior technology over other drying methods such as tray and oven dryers. Because of its appeal, accurate fluidized bed drying modeling is desired. The motivation for this work is to address the need for evaluating fluidized bed drying effectiveness.

All major areas of chemical engineering fundamentals are required to describe the physics in fluidized bed drying. These include:

1. Momentum transfer describes the flow of gas through the particles and the incipience of fluidization along with the flow pattern of the particles in and out of the bed.
2. Heat transfer describes the heating of particles by both gas and internal coils.
3. Mass transfer describes the diffusion of the liquid (almost always water) from the particle pores to the particle surface and then to the gas phase.
4. Thermodynamics describe the potential for water to enter the gas phase and also describe the kinetics.

A large number of independent variables such as particle density, size, shape, permeability, and hygroscopicity can influence drying behavior. Fluidized bed drying is one of the most successful methods, which has been used since 1960s. In fluidized bed, dryer moist particles are suspended in a hot air or stream.

The fluidized-bed dryer possesses many significant features over the conventional packed-bed or moving bed dryer these include the following:

(i) Drying gas is locally mixed intensively during its passage through the bed, Consequently the rate of mass and heat transfer between the gas and solids are high and favorable transportation conditions to carry out continuous operation, are utilized at drying processes, too.

(ii) The extremely rapid heat transfer enables a relatively high inlet gas temperature to be used.

(iii) The time of drying is relatively short.

1.1 FLUIDISED BED DRYER

Fluid bed dryer is an entirely different kind of pneumatic conveying dryer. Fluid-bed drying permits continuous, large-scale drying of foods without over drying. The high heat transfer rates make it an economical process, and the lack of mechanical parts ensures low maintenance costs. The rapid mixing in the bed provides nearly isothermal drying conditions. In batch operation products are mixed by fluidization and this leads to uniform drying. In continuous dryers, there is a greater range of moisture contents in the dried product, and bin dryers are therefore used for finishing. Fluidized-bed dryers are limited to small particulate foods that are capable of being fluidized without excessive mechanical damage (e.g. peas, diced or sliced vegetables, grains powders or extruded foods). These considerations also apply to fluidized-bed freeze dryers and freezers.

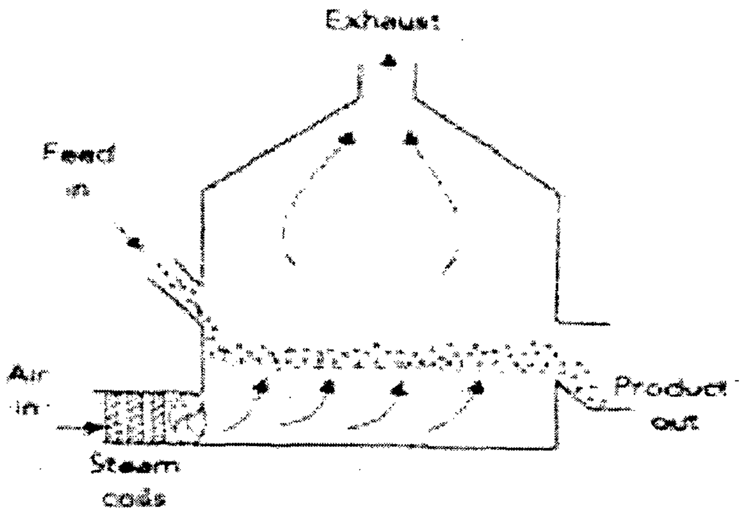

Fig.1.1. Fluidized-bed dryer

There are various fluid bed designs:

1.2 VIBRATED FLUID BED: If the product to bed dried does not fluidize in a standard fluid-bed Dryer because the particle distribution is too wide or the particles break up due to their low strength, or if they are sticky, thermoplastics, or pasty, vibrated fluid-bed dryer may be applicable. A long, rectangular, narrow drying chamber is vibrated at 5 to 25 Hz. The air velocity within the dryer can be as low as 20 % of the minimum fluidization velocity. The large particles are transported through the dryer by the vibration of the dryer. The vibration provides a gentler means of transportation than vigorous of agitation in stationary fluid-bed dryers. Vibrated fluid-bed dryers typically dry such products as milk, whey, cocoa, and coffee.

1.3 FLUID -BED GRANULATION: A second variation of fluid-bed drying is fluid-bed granulation. A binding liquid is sprayed into the fluidized bed of granules, causing the particles to agglomerate. The process is advantageous because it is not dust producing. The average particle size produced ranges from 0.5 to 2 mm. The process has widespread use in the pharmaceutical industry.

1.4 SPOUTED BED DRYER: When the particles to be dried are larger than 5 mm and are not readily fluidized in a conventional fluid-bed dryer, a spouted bed dryer is employed. The drying air enters the drying chamber at the centre of the conical bottom. The particles move in a cyclic fashion through the dryer. As they travel upward in the centre, they are carried by the incoming air stream and fall downward at the periphery of the chamber. The advantages of spouted bed dryers are the excellent solids mixing and heat transfer rates. Spouted bed dryers have successfully dried- heat sensitive goods such as wheat and peas.

1.5 MECHANICALLY AGITATED FLUID -BED DRYER: A combination fluid-bed and flash dryer is used to wet cakes was developed to conserve energy costs. The wet cake is fed directly via a screw conveyor. Once in the drying chamber, a mechanical agitator breaks up the particles while air is introduced to fluidize the small particles. Dry particles are carried to the exhaust system by the fluidizing system. Pastes of pigments and dyes are dried industrially using this method.

1.6 CENTRIFUGAL FLUID-BED DRYERS: Rapid pre-drying of sticky foods with high moisture content has been done in centrifugal fluid -bed dryers. Diced, sliced, and shredded vegetables that are difficult to fluidize and too heat sensitive to dry in conveyor dryers are also dried in centrifugal fluid-bed dryers. The cylindrical dryers rotate horizontally while air flows in to the chamber through the perforated wall. The solids alternate between fluid-bed and fixed bed configuration as the dryer rotates.

1.7 FLUIDIZED SPRAY DRYER: Another alternative for hygroscopic and thermoplastic foods is the fluidized spray dryer. A fluid-bed chamber is installed directly in the spray-drying chamber. The fluidizing air is led to the bottom of the drying chamber. The combination of partially dried and dried products and allows agglomeration to take place. Small particles entrapped in the air are recycled from the exhaust system to the drying chamber. The combination of spray and fluid drying provides very efficient use of the drying chamber and produces agglomerated products with low bulk density and good initializing characteristics.

The lists below are the characteristics that generally describe the materials suitable for fluid-bed drying:

1. The average particle size must be between 20 μm and 10 mm to avoid channeling and slugging. Particles smaller than 20 μm tend to lump together because of their large surface area.
2. The particle size distribution must be narrow to ensure that the majority of the particles are fluidized and few are lost by entrainment in the air.
3. For proper fluidization, especially of larger particles, the particles should be spherical.
4. If any lumps are present in the fluid material, they must break up readily once in the dryer, to retain fluidity in the bed.
5. The particles must be strong enough to withstand vigorous mixing in the bed.
6. The final product must not be sticky at the fluid-bed exit temperature.

***1.8 ADVANTAGES OF FLUIDIZED BEDS*:**

1. The smooth liquid like flow of particles allows continuous automatically controlled operation with the ease of handling.
2. The rapid mixing of solids leads to nearly isothermal conditions throughout the reactor; hence the operation can be controlled simply & reliably.
3. The circulation of solids between two fluidized beds makes it possible to transport the vast quantities of heat produced or needed in large reactors.
4. It is suited to large scale operations.
5. Heat & mass transfer rates between gas and particles are high when compared with other modes of contacting.
6. The rate of heat transfer between a fluidized bed and an immersed object is high; hence

heat exchangers within fluidized beds require relatively small surface areas.

1.9 DISADVANTAGES OF FLUIDIZED BEDS :

1. It is difficult to describe the flow of gas with its large deviations from plug flow and the by passing of solids by bubbles, representing an inefficient contacting system.
2. Friable solids are pulverized and entrained by the gas then they must be replaced.
3. Erosion of pipes and vessels from abrasion by particles can be serious.

1.10 OBJECTIVE OF OUR PRESENT STUDY

1. To develop the simple mathematical model.
2. To solve the mathematical model by using Matlab software.
3. To validate the model with the available experimental results in the literature.
4. To study the effect of various parameter on the performance of the model.

LITERATURE REVIEW

Fluidized bed dryer have promising applications in many industrial processes. Many papers have been published on the development of fluidized bed dryer by different authors. Useful information about the fluidized bed dryer has been given. These papers have been reviewed and brief description of their work has been presented in this chapter.

Mori and Wen (1975) has developed a model which considers Bubble size as one of the most important parameters in the design and simulation of a fluidized-bed reactor. A correlation of the bubble size and growth in fluidized beds of various diameters is developed. A maximum bubble diameter determined from the bubble coalescence is incorporated in the correlation to relate the effect of the bed diameter on the bubble size. Experimental data of bubble size reported are used to develop and test the validity of the correlation. The bubble diameters calculated using this correlation show good agreement with the observed bubble diameters. A correlation of bubble diameter for fluidized beds of various sizes included pilot scale is presented. Although many correlations for estimation of bubble diameter in fluidized beds are available, none of these correlations can predict the effect of the bed diameter on the bubble diameter. In this paper, the bubble size and bubble growth rate are examined in light of the bed diameter and the design of distributor plates. A semi-empirical equation for bubble growth in fluidized beds of various sizes including pilot plant scale is presented.

The proposed bubble growth correlation has the form

$$\frac{(D_{BM}-D_B)}{(D_{BM}-D_{B0})}=\exp\left(-\frac{0.3h}{D_t}\right)$$

Initial bubble diameter formed at the surface of the perforated plate is calculated from

$$D_{B0}=0.347\left[\frac{A_t(u_0-u_{mf})}{n_d}\right]^{2/5}$$

The value of D_{B0} for porous plate distributor can be evaluated from

$$D_{BM}=0.652\{A_t(u_0-u_{mf})\}^{2/5}$$

Various correlations for estimating bubble diameters in fluidized beds have appeared in the literature and are summarized below. Most of these correlations are derived from data obtained from relatively small diameter beds. Therefore these correlations are not useful in predicting the change in the bubble diameter when the bed diameter is changed.

author	year	correlation
Yasui et al.	1958	$D_B = 1.6_{ppdp}\left(\frac{u_0}{u_{mf}} - 1\right)^{0.63} .h$
Kato and wen	1969	$D_B = 1.4_{ppdp}\left(\frac{u_0}{u_{mf}}\right)h + D'_{B0}$
Park et al.	1969	$D_B = 33.3dp^{1.5}\left(\frac{u_0}{u_{mf}} - 1\right)^{0.77} h$
Whitehead etal.	1967	$D_B = 9.76\left(\frac{u_0}{u_{mf}}\right)^{0.33(0.32h)^{0.54}}$
Rowe et al.	1972	$D_B = -A + Bh + C\left(\frac{u_0}{u_{mf}}\right) + Dh\left(\frac{u_0}{u_{mf}}\right) + E\left(\frac{u_0}{u_{mf}}\right)^2$
Geldart	1971	$D_B = D'_{B0} + 0.027(u_0 - u_{mf})^{0.94} h$
Chiba et al.	1973	$D_B = D_{B0}"\{2^{7/6} - 1)(h - hB_0)/D_{B0}" + 1\}^{2/7}$ for $h < h_{k^0}$

Tab.2.1. Summary of correlations for bubble diameter in fluidized beds

Broadhurst and Becker (1975) had made comprehensive investigation on the boundaries of the regime of bubbling aggregative fluidization. Experiments were done with sand, glass beads, clover seed, and iron shot fluidized with helium, air, and freon-12 in columns 2.5, 5, 10, and 21 cm in diameter. Bed heights ranged from 1 to 60 column diameters, particle diameters from 0.07 to 1.1 mm, particle densities from 1300 to 7600 kg/m^3, and gas densities from 0.17 to 5.2 kg/m^3. Correlations are presented for the void fraction at the minimum bubbling point and for the superficial fluid velocity at the points of minimum fluidization, minimum bubbling, and minimum slugging. His results show that the superficial fluid velocity at the point of minimum slugging depends strongly on the ratio of bed height and column diameter. This dependency does not appear in the hitherto accepted criteria for the occurrence of slugging, and it is evident that these generalizations were based on insufficient data. The ratio of the gas and particle density also exerts an effect, small but significant, and previously unrecognized. The minimum slugging velocity increases with increasing particle diameter but not as rapidly as the minimum bubbling velocity. The difference is relatively small for large particles, and the regime of good aggregative fluidization is correspondingly smaller in extent. The minimum slugging velocity decreases with increasing bed height, but the rate of decrease is smaller for large particles than for small ones, and smaller for dense particles than for light ones. The minimum fluidization velocity tends to be slightly larger than the minimum bubbling velocity but the differences are practically unimportant.

Grace (1980) a non-interfering technique has been used to measure the concentration of ozone in pairs of bubbles injected into a bed of inactive 390 μm glass beads fluidized by ozone-free air. The transfer of the ozone tracer from the bubble phase to the dense phase is enhanced when compared to the transfer from isolated bubbles in the same particles and the same column. Bubble growth is also greater for the case where pairs of bubbles are introduced than when bubbles are present in isolation. Enhancement of inter phase mass transfer for interacting bubbles in the present work and in previous studies increases with particle size and can be explained in terms of enhancement of the through flow (or convective) component of transfer while the diffusive component remains unaltered. This mechanism leads to new equations for estimating inter-phase mass transfer in freely bubbling fluidized beds.

Palancz (1982) has developed a mathematical model for continuous drying process in a fluidized bed-dryer. To describe the heat and mass transfer in gas phase, a Kunii-Levenspiel type, three phase model representing a dilute (bubble) phase, interstitial gas phase and solid phase, is employed. The dilute phase is assumed to be in plug flow while the interstitial gas as well as the solid particles is considered to be perfectly mixed. Using a simplified lumped model for single solid particle, the heat and mass transfer between the interstitial gas and solid phase as well as the heat transfer between the solid phase and the dryer-wall can be taken into account during the whole drying process as warm-up, constant and falling-rate periods. Numerical computation based on this model was done to study the effects of the process parameters as particle and bubble-size, gas velocity, inlet gas temperature and residence time, on the moisture content of the solid outlet. Their model can be employed for simulating drying process in fluidized bed as well as for dimensioning dryer equipments.

Lai and Chen (1985) has developed a fairly rigorous mechanistic model of a continuous fluidized-bed dryer has been developed. It depicts the dynamic interactions between gaseous and solid phases in detail. The performance of the dryer has been simulated numerically based on the model. The effects of the operating parameters on the performance characteristics of the dryer have been investigated. Their parameters study includes the superficial gas velocity, the inlet temperature of the drying gas, the mean residence time of solids and the dryer-wall temperature. The results of simulation based on the present model are compared with those based on an existing model. This comparison shows that the former is a substantial improvement over the latter.

Boyle (1990) had proposed a theory for the modeling of solid particles in fluidized beds based on ideas in the theory of interacting continua. The theory is capable of predicting the behavior of the mixture in the two extremes. That is, in one limit, as the concentration of solid particles becomes small, the theory reduces to the classical theory of incompressible viscous fluid. In the other limit, as the effect of the interstitial fluid becomes negligible, the theory reduces to the flow of incompressible granular materials. The mixture is considered to be made up of a linearly viscous fluid and granular materials. The stress tensors for the solid particles are derived using a modified version of Enskog's dense gas theory. The normal-stress effects that are observed experimentally in granular materials are predicted in this theory due to a solids fraction gradient. The dependency of the granular stress tensor on the solids fraction gradient arises by requiring that the correlation function that links the two-particle distribution function to the two single-particle distribution functions be the contact value for the radial distribution function of a non-homogenous, hard sphere fluid. The interaction force is assumed to have contributions from density gradients, relative velocity and relative acceleration.

Liedy and Hilligardt (1991) Fluidized bed driers are used in many large-scale processes. In process selection, an estimate of size and operating parameters on the basis of laboratory data is desirable, in order to obtain a cost estimate for the production plant as soon as possible. They developed a model of fluidized bed dryer. Their model allows for the influence of bubbles in fluid dynamics. Heat and mass transfer coefficients between particles and suspending gas are determined from a simple discontinuous laboratory experiment. The transport coefficients between suspending gas and bubbles can be calculated by means of correlations from the literature. Their procedure is used for scaling up the discontinuous operation. In a further step, the behavior of continuously operating fluidized bed driers was modeled. The core piece of this modeling is the calculation of the distribution function which indicates, as a function of the moisture content, how the quantity of product is distributed in a continuously operated stirred vessel. As in scaling up, only easily determined laboratory data are required for the entire calculation of the continuous operating behavior. Starting from simple discontinuous laboratory experiments, a fairly accurate cost estimate for discontinuously and continuously operated fluidized bed drying processes can be made by means of the method described in their paper.

Molerus and Burschka (1994) in a gas fluidized bed, heat to and from a heat exchanger surface can be transferred by the gas and/or particle convection. Despite more than 40 years of intensive research on this topic, the contribution through particle convection remains inadequately described, while the gas convective component has been straightforward to predict. In Part 1 of their paper, the pulsed light method of tracing particles in a fluidized bed close to a wall has been introduced, allowing a better understanding of how particle convective heat transfer works. In Part 2 they proposed a correlation, which allows prediction of the heat transfer coefficient in dependence of the superficial gas velocity. The correctness of their prediction is tested by comparison with more than 20 measurements covering the following range of system data and operational conditions:

Particle size 74 - 4000 μm

Particle density 26 - 11,800 kg m^{-3}

Gas pressure 0.03 - 2 MPa

Bed temperature 290 - 1050 K

Excess gas velocities up to 2.5 ms $^{-1}$.

In the investigated temperature range of 290 - 1050 K there appears to be no significant contribution to the heat transfer due to radiation.

Wiman and Almstedt (1998) the hydrodynamics have been studied in a cold, freely bubbling, pressurized fluidized bed. The bed has a cross-section of 0.2 mX0.3 m and was operated at pressures between 0.1 and 1.6 MPa and at excess gas velocities of 0.2 and 0.6 m/s. The bed material was silica sand with a mean particle diameter of dp = 0.45 mm. Comparisons were made with previous results obtained with particles of dp = 0.7 mm. The hydrodynamic results are similar for the two different particle sizes when plotted vs. the excess gas velocity. The results also show that the bed expansion, bubble rise velocity, bubble volume fraction and visible bubble flow rate fall on single curves if plotted vs. a dimensionless potentially available drag force, while the bubble frequency, the mean pierced length and the through-flow velocity of gas through the bubble do not. The dimensionless drag force is a suitable scaling parameter as long as the particles do not respond to the gas-phase velocity fluctuations and as long as the dense phase does not expand. At high pressures, an increased gas particle interaction, in combination with turbulent fluctuations in the gas phase, can be used to explain the increased bubble instability, with a corresponding increased bubble splitting and dense phase expansion. The gas particle interaction also increases with decreasing particle size, which may help explain the maximum stable bubble size for group A particles.

Zhao and Chen (1999) has developed a coupled heat and mass transfer model for batch fluidized-bed drying of moist porous particles considering the temperature, moisture saturation and pressure distributions in the particle. Their model equations are solved numerically based on physical properties of apple. The heat and mass transfer mechanisms in the fluidized-bed drying process are analyzed. Their results show that capillary flow and vapor diffusion play different roles in moisture transfer in the particle during different drying periods. The internal heat transfer can greatly affect the drying process while the effect of gas pressure distribution is insignificant. Due to the coupled effects between gas and particles, the state of gas in the fluidized-bed changes substantially along the bed height and affects the heat and mass transfer in the particle significantly. A new parameter called bed area factor is derived and analyzed. It is important in determining the drying efficiency in the design and operation of fluidized-bed dryers. The effects of particle parameter and inlet gas conditions on heat and mass transfer in the fluidized-bed drying process are discussed through the analyses of drying characteristics.

Temple and Boxtel (1999) has developed a mathematical model for fluidized-bed drying of tea based on differential equations and drying properties of tea, which takes into account equipment dimensions and models the changes in the air used for drying. The model can be used for simulation of batch drying, and for continuous drying, it is able to simulate the start-up phase of operation. Simulations have been carried out to illustrate the characteristics of various types of dryer, demonstrating that the model has broad application. The simulation model was experimentally validated on a thin-layer drying test rig, and on fluidized-bed dryers. To account for the loss of efficiency between thin layer and fluidized-bed, an efficiency factor of 0.6 was used, which was appropriate for, and validated on, an experimental batch dryer, a pilot-scale continuous dryer and a commercial dryer in a tea factory. The developed simulation model is useful for design, operational setting and control system design. The constant rate drying phase is shown to be a property of the drying air rather than the material being dried.

The following assumptions are made in their model:

1. The fluidized-bed exhaust is open to the atmosphere, so the top is at atmospheric pressure.
2. The pressure differential across the bed of tea is small, so drying is at constant pressure.

3. No energy is gained or lost in the dryer, so the drying process is adiabatic.
4. For a constant weir height, bed loading is constant while dhool is being fed at a greater rate than evaporation.
5. Well-mixed fow of dhool from the inlet to the outlet (plug flow can be approached by the series connection of the well-mixed systems).
6. Plug flow of air from the inlet at the bottom to the exhaust at the top.
7. Complete mixing of air and dhool particles (no bubbling fluidization).
8. Heat exchange between the particle and air is complete so that air exhaust temperature equals particle temperature.
9. Mass of the air resident in the bed is negligible.

Templel & Boxtel (1999) in their paper describe the experiments used to determine the kinetics of tea drying. New thin layer drying apparatus was designed and built to measure the very high rates of drying found at the start of drying, and their results show that the Lewis equation satisfies. The drying rate constant proved to be a linear function of temperature and airflow rate, indicating that tea drying is not only diffusion limited but also a function of convection. Their results were validated on independent experiments. Results from over 170 thin layer drying experiments were used to derive a drying rate factor for the Lewis drying equation. The value for the rate factor was confirmed by independent experiment. The drying rate factor k for macerated tea particles was found to be dependent on air temperature as expected, and was observed to be strongly dependent on airflow velocity, in contrast to the results from other research. The reason why tea dries in a way different from most other agricultural produce may be because of the small particle size, the breakdown in cellular structure and the high concentration of soluble substances in the free cell sap. A single function describes the whole process of thin layer drying of tea from 70% m.c. w.b. down to 3%. The drying rate is directly proportional to the superficial airflow and the air temperature. The absence of a constant rate period is in accordance with the published results.

Temple & Boxtel (1999) work characterizes the fluidization parameters for tea particles. They developed Relationships for minimum fluidizing velocity, pressure drops across the bed and bedplate and bed expansion. They found different bedplate designs only affect the fluidization by the range of loads that fluidize well on each bedplate. The values determined in their study can be used for design, operation and control of tea dryers. Limitations on the range of permissible air velocities and bed loadings were determined. For four types of bedplate with dry tea, the minimum air velocity for fluidization was determined to be between 0.35 and 1.2 m/s. Elution of light particles was observed soon after the onset of fluidization, reducing the acceptable air flow velocities into a narrow range. Measurements on an industrial dryer showed that slightly higher air velocities were required for tea at higher moisture contents; an air velocity of 1.3 m/s with the tea at a moisture content of 72% w.b. being required for normal operation, falling to 0.9 m/s at 3% w.b. Their experiments showed a dependence of the pressure drop across the layer of the fluidized material at minimum fluidizing velocity to be linearly related to bed load. The bed expansion is also a linear function of load and an exponential function of the air flow velocity. Bedplate variables were also found to influence the stability of fluidization. A smaller open area percentage allowed fluidization over a wider range of bed loadings. The pressure drop across the bedplate was found to vary with the square of velocity. Limits to fluidization were found at higher bed loadings, when channeling occurred.

Wang and Rhodes (2002) their paper presents a study of particle residence time near the walls of gas fluidized beds by DEM simulation. The simulation experiments were performed in two beds, one of 50 mm X 50 mm cross-section and the other of 90 mm X 90 mm cross-section. The particles used were 0.5 and 1 mm in diameter and 2650 kg/m^3 in density. The number of particles used was 600,000 and 500,000 for simulations of the 0.5 and 1 mm diameter particles, respectively. The advantage of their approach is that it enables an unprecedented amount of information pertaining to the motion of individual particles near the walls of a fluidized bed to be obtained. These include the distribution of particle residence time, mean residence time, contact frequency, and contact distance at the walls. They examined the variations of particle residence time with particle size, gas velocity, and wall position. They highlighted the significance of the results to modelling of particle-to-wall heat transfer in fluidized beds.

Syahrul and Hamdullahpur (2002) A thermodynamic analysis of the fluidized bed drying process of large particles is performed to optimize the input and output conditions. Energy and exergy models were used for the study. The effects of the hydrodynamic and thermodynamic conditions such as the inlet air temperature, the fluidization velocity and the initial moisture content on the energy efficiency and the exergy efficiency were analyzed. The analysis was carried out using two different materials, wheat and corn. It was observed that the thermodynamic efficiency of the fluidized bed dryer was the lowest at the end of the drying process in conjunction with the moisture removal rate. The inlet air temperature has a strong effect on thermodynamic efficiency for wheat, but for corn, where the diffusion coefficient depends on the temperature and the moisture content of particles, an increase in the drying air temperature did not result in an increase of the efficiency. Furthermore, the energy and exergy efficiencies showed higher values for particles with high initial moisture content while the effect of gas velocity varied depending on the particles. A good agreement was achieved between the model predictions and the available experimental results.

Lib and Kuipersa (2003) had studied on the occurrence of heterogeneous flow structures in gas-particle flows seriously affects gas–solid contacting and transport processes in dense gas-fluidized beds. A computational study, using a discrete particle method based on Molecular Dynamics techniques, has been carried out to explore the mechanisms underlying the formation of heterogeneous flow structures. Based on energy budget analyses, the impact of non-linear drag force on the flow structure formation in gas-fluidized beds has been examined for both ideal particles (elastic collision, without inter-particle friction) and non-ideal particles (inelastic collision, with inter-particle friction). Meanwhile, the separate role of inter-particle inelastic collisions, accounted for in the model via the restitution coefficient (e) and friction coefficient (μ), has also been studied. It is demonstrated that heterogeneous flow structures exist in systems with both non-ideal particle-particle interaction and ideal particle-particle interaction. The heterogeneous structure in an ideal system, featured with looser packing, is purely caused by the non-linearity of the gas drag, the stronger the non-linearity of the gas drag force with respect to the voidage, the more heterogeneous flow structures develop. A weak dependence of drag on the voidage produces a homogenous flow structure. Collisional dissipation dramatically intensifies the formation of heterogeneous flow structures after the system equilibrium breaks.

Patil and Kuipers (2004) have developed correct prediction of spontaneous bubble formation in freely bubbling gas–solid fluidized beds using Eulerian models, strongly depends on the description of the internal momentum transfer in the particulate phase. In this part, the comparison of the simple classical model, describing the solid phase pressure only as a function of a solid porosity by an empirical correlation and assuming the solid phase viscosity constant, which is referred to as the constant viscosity model (CVM), with the more fundamental model based on the kinetic theory of granular flow (KTGF), in which the solid phase properties are described in much more detail in terms of instantaneous binary particle–particle interactions, has been extended for freely bubbling fluidized beds. The performance of the KTGF and the CVM in predicting the hydrodynamics of freely bubbling fluidized beds has been compared with experimental data and correlations taken from the literature. In freely bubbling fluidized beds at relatively low gas velocities, bubble formation is initiated by inelastic particle–particle interactions. When accounting for the dissipation of granular energy by particle collisions, the KTGF predicts much larger bubbles with a much sharper interface in comparison to the CVM. The average bubble size distribution predicted by the KTGF showed better agreement with correlations as well as experimental data from the literature. Although both models showed an increase in the predicted average bubble size with increasing superficial gas velocities, the discrepancy in the predicted bubble size becomes smaller, indicating the growing importance of the gas particle interactions in the bubble formation process at higher gas velocities. The rise velocity predicted by the KTGF and the CVM is approximately the same and in good agreement with correlations available in the literature. Since the KTGF predicts somewhat larger bubbles, also the predicted visible bubble flow is higher in comparison to the CVM. In very dense regions in the fluidized bed the KTGF based on instantaneous binary collisions needs to be extended for additional frictional stresses in addition to the kinetic and Collisional transport mechanisms. The extra frictional stresses were implemented via a relatively

simple semi-empirical closure model and proved to have a significant influence on the predicted bubble size, rise velocity and visible bubble flow rate, where the model predictions strongly depend on the empirical constants. To further enhance the performance of the KTGF to describe the hydrodynamics of freely bubbling beds a more fundamental description of the frictional stresses on the particle
level should be incorporated.

Garnavi and Hashemabadi (2006) in their work, a numerical simulation of a fluidized bed dryer based on the two-phase theory of fluidization has been proposed. Solid particles in the emulsion phase are considered lumped and in the bubble phase is assumed plug while in the emulsion phase is considered totally mixed. Moreover, the bubble size variations along the bed height are taken into consideration. Influence of the superficial gas velocity, input temperature of drying gas, particle size and mean residence time of solid particles on the drying process have been reported. The simulation results show an improvement to the prediction of other models that consider uniform size bubble and other simplification assumptions.

Deen and Kuipers (2006) this paper reviews the use of discrete particle models (DPMs) for the study of the flow phenomena prevailing in fluidized beds. DPMs describe the gas-phase as a continuum, whereas each of the individual particles is treated as a discrete entity. The DPMs accounts for the gas–particle and particle–particle interactions. This model is part of a multi-level modeling approach and has proven to be very useful to generate closure information required in more coarse-grained models. In this paper, a basic DPM, based on both the hard and soft-sphere approaches is described. The importance of the closures for particle–particle and gas–particle interaction is demonstrated with several illustrative examples. Finally, an outlook for the use of DPMs for the investigation of various chemical engineering problems in the area of fluidization is given.

Yang and Bing (2006) Current worldwide commercial activities in converting natural gas to fuels and chemicals, or gas-to-liquids technology use slurry bubble column reactors

with column sizes considerable larger than that currently in practice. Such commercial activities have prompted further fundamental research interest in fluid and bubble dynamics, transport phenomena and the scale up effects of three-phase fluidization systems. The fundamental behavior of particular relevance to these activities is associated with the elevated temperature and pressure conditions. This review attempts to summarize the salient characteristics of liquid, bubbles, and particles and their interactive behavior and dynamics in the process of bubble formation and bubble rising in gas–liquid–solid fluidization systems. Measurement techniques including both intrusive techniques such as the probes, and non-intrusive techniques such as tomography, that are used to study fluid and bubble properties in gas–liquid and gas–liquid–solid systems, are illustrated. Governing mechanisms of bubble–particle collision and bubble breakup are discussed. The state of-the-art computational techniques, that consider both the discrete and the continuum approaches for movement of the particle and bubble phases along with the discrete simulation results, are presented. Of particular emphasis is the effect of pressure and temperature on the fluid and bubble dynamics in three-phase fluidization.
Numerical simulation of fluid bed drying based on two-fluid model and experimental validation

Assari and Saffar-Avval (2006) developed a mathematical model for batch drying based on the Eulerian ''two-fluid models''. The two-dimensional, axis-symmetrical cylindrical equations for both phases were solved numerically. Their governing equations were discretized using a finite volume method with local grid refinement near the wall and inlet port. The effects of parameters such as inlet gas velocity and inlet gas temperature on the moisture content, temperature of solid and gas at the outlet were shown. This data from the model was compared with that obtained from experiments with a fluidized bed and found to be in reasonably good agreement.
Baker and Khan (2006) have formulated a mathematical model of plug flow fluidized bed dryers. Their model was based on analytical equations previously derived to simulate well-mixed fluidized bed dryers, combined with axial dispersion theory. It was implemented on Microsoft Excel 2000; the calculations were fully automated with the aid of a macro programmed in Visual Basic. The model outputs include moisture,

temperature and specific energy Consumption profiles along the length of the dryer, the condition of the outlet streams, and the overall specific energy consumption. The effects of dryer geometry and the principal operating parameters were investigated and followed logical trends. Dispersion had a negligible effect on the results under the industrially realistic conditions employed in the simulations. The outlet moisture content of the solids was found to depend on the difference between the temperature and dew point of the exhaust air and the drying kinetics. Specific energy consumption increased with decreasing outlet moisture content and was in good agreement with values calculated assuming an ideal adiabatic dryer.

Croxford and Gilbertson (2006) Bubbling fluidized beds are used for a wide variety of industrial processes. As such it is desirable to be able to specify the conditions within the bed. These conditions can be subject to unwanted change in areas such as feedstock or fluctuations in process settings such as gas flow. Their paper shows how pressure measurements can be used to characterize changing conditions within a three-dimensional bubbling fluidized bed. These characterization techniques are then used to show that a linear controller can control the conditions within a bubbling bed. This control is demonstrated to be robust, being insensitive to the gas flow conditions, controller gains and location at which the characterization measurement is made.

MATHEMATICAL MODELLING

3.1 Model Development

Consider a bubbling Fluidized-bed dryer with continuous supply and removal of solid particles. The hot inlet gas-stream fluidizes the bed as well as provides the drying medium for removing the moisture content of the particles. The dryer is schematically represented by Fig.1.

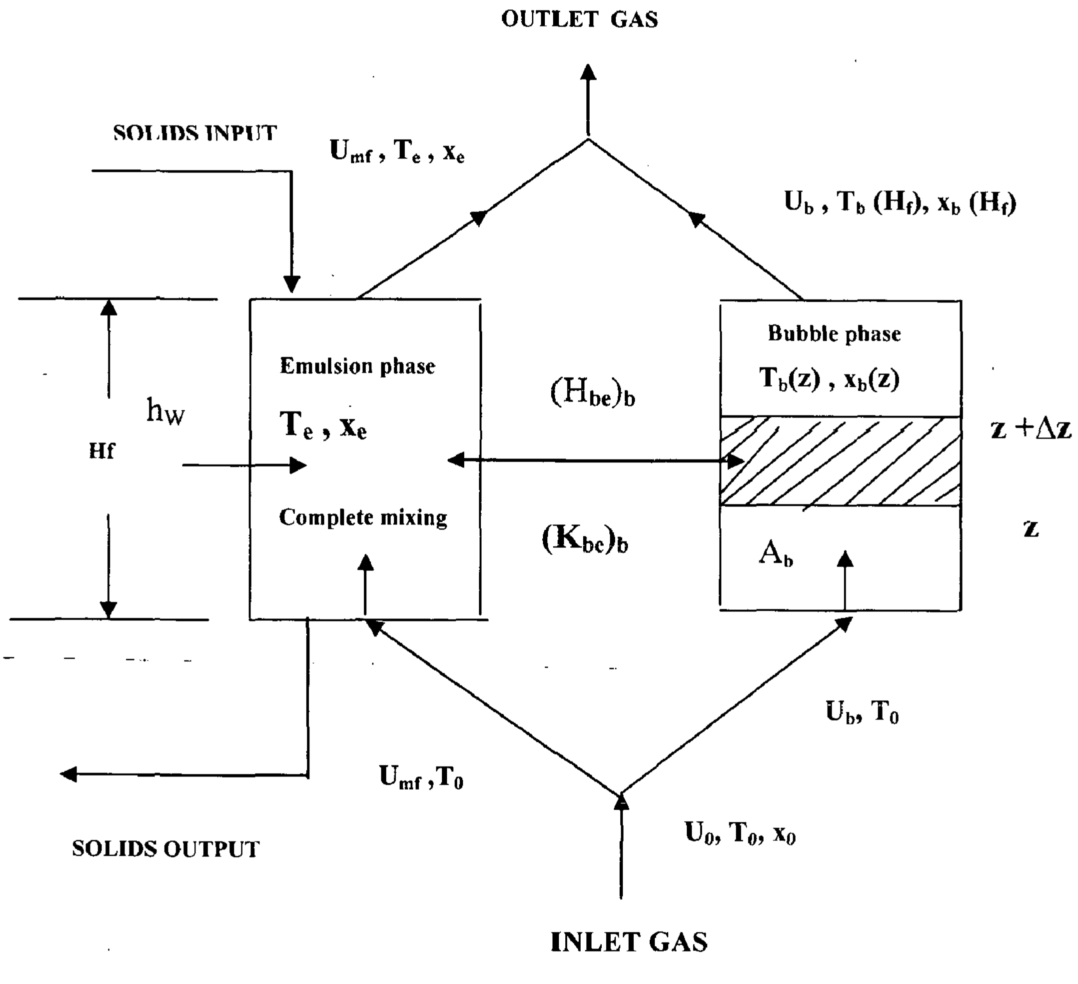

Fig.3.1. Schematic diagram of continuous drying in the fluidized bed

In this model it is assumed that the dryer can be divided into two phases: a dilute phase or bubble phase, and an emulsion phase, which consists of gas and solid particles. The emulsion phase remains at the minimum fluidization condition while the excess flow of fluidizing fluid passes through the bed as bubbles. In addition the bubble size and bubble growth rate are examined in the light of the bed diameter.

The aim of the present study is to develop a numerical simulation with the above simplifications. The model is able to predict and determine the average moisture content and temperature of the output solid particles. In addition, this model predicts profiles of these variables with time.

3.2 Assumptions

1. The bubble phase is solid-free.
2. The movement of bubbles through the bed is of plug flow.
3. The clouds surrounding the rising bubbles are very thin and, therefore, the bubble phase exchanges mass and energy only with the emulsion gas.
4. The emulsion gas and solid particles are perfectly mixed.
5. Solid particles are added and removed at a constant rate.
6. The inlet temperature and moisture content of solids are assumed to be uniform.
7. The internal resistance of solids to mass and heat transfer is negligible.
8. Particles are considered to be uniform in size, shape and physical properties.
9. The temperature and moisture content of each particle depend on its age, t,, that is, the length of its stay in the dryer.
10. The residence time distribution function for solids under a steady-state condition is

$$f(t_s) = \left(\frac{1}{\bar{t}_s}\right)\exp\left(-\frac{t_s}{\bar{t}_s}\right)$$

11. Viscous dissipation is negligible.
12. The changes in the physical properties of both solids and drying gas due to the change of temperature are negligible.

3.3 Mass conservation equations

A) Bubble phase: A steady state moisture balance around the bubble phase

$$x_b = x_e - (x_e - x_0)\exp\left[-\frac{(K_{be})_b\delta_b}{U_b}z\right] \quad \text{.........................} \quad (1)$$

The boundary condition for the above equations is

$$x_b = x_0 \quad \text{at} \quad z = 0$$

B) Moisture balance around the entire emulsion gas

$$\rho_g\left(\frac{U_{mf}}{H_f\delta_b}\right)(x_e - x_0) = \rho_g(K_{be})_b(\bar{x}_b - x_e) + \frac{(1-\varepsilon_{mf})(1-\delta_b)}{\delta_b}\frac{6}{d_p}\sigma(\overline{x_p^*} - x_e) \quad \text{........ (2)}$$

C) Single solid particle: A steady state moisture balance around the single solid particle

$$\rho_s\frac{dx_p}{dt_s} = -\left(1 + \frac{\rho_s}{\rho_w}x_{pc}\right)\frac{6}{d_p}\sigma(x_p^* - x_e) \quad \text{.................. (3)}$$

The boundary condition for the above equations is

$$x_p = x_{p0} \text{ at } t_s = 0$$

3.4 Energy conservation equations

(A) Bubble phase: A steady state energy balance around the bubble phase

$$\frac{dT_b}{dz} = \frac{T_e - T_b}{(c_g + c_{wv}x_b)}\left[\frac{(H_{be})_b\delta_b}{U_b\rho_g} + \frac{\delta_b(K_{be})_b(x_e - x_0)c_{wv}}{U_b}\exp\left(-\frac{(K_{be})_b}{U_b}\delta_b z\right)\right] \quad \text{............... (4)}$$

Boundary conditions

$$T_b = T_0 \text{ at } z = 0;$$

(B) Emulsion gas: A steady state energy balance around the emulsion gas

$$\frac{\rho_g U_{mf}}{H_f}(c_g + c_{wv}x_0)(T_e - T_0) = \delta_b(H_{be})_b(\bar{T}_b - T_e) + (1-\delta_b)(1-\varepsilon_{mf})\frac{6}{d_p}(\bar{T}_p - T_e)[c_{wv}\sigma(\overline{x_p^*} - x_e) + h_p]$$

$$\text{............. (5)}$$

(C) Single solid particle: A steady state energy balance around the single solid particle

$$\rho_s(c_p + x_p c_w)\frac{dT_p}{dt_s} = \left(1 + \frac{\rho_s}{\rho_w}x_{pc}\right)\frac{6}{d_p}[h_p(T_e - T_p) - \sigma(x_p^* - x_e)(c_{wv}T_e - c_w T_p + \gamma_0)]$$

$$\text{.............. (6)}$$

Boundary conditions

$$T_p = T_{p0} \text{ at } t_s = 0 ;$$

3.5 Correlations

The diameter of the bubble has been given by

$$D_B = 33.3dp^{1.5}\left(\frac{u_0}{u_{mf}}-1\right)^{0.77} h$$

The minimum fluidization velocity can be approximated by the following formula

$$\frac{d_p U_{mf}\rho_g}{\mu_g} = \left((33.7)^2 + 0.0408\frac{d_p^3\rho_g(\rho_{ws}-\rho_g)g}{\mu_g}\right)^{0.5} - 33.7$$

The superficial velocity through the bubble phase

$$U_b = U_0 - U_{mf}$$

The bubble rise velocity is given by

$$U_{br} = 0.711(gd_b)^{0.5}$$

The fraction of fluidized bed consisting of bubble is given by

$$\delta_b = \frac{(U_0 - U_{mf})}{(U_0 - U_{mf}) + U_{br}}$$

The void fraction at minimum fluidizing conditions

$$\varepsilon_{mf} = 0.586\phi_s^{-0.72}\left[\frac{\mu_g^2}{\rho_g(\rho_{ws}-\rho_g)gd_p^3}\right]^{0.029}\left(\frac{\rho_g}{\rho_{ws}}\right)^{0.021}$$

The effective diffusion coefficient of drying gas

$$D_{eff} = \varepsilon_{mf} D_g$$

The coefficient of gas interchanges between the bubble and the emulsion phase based on the volume of the bubbles

$$(K_{be})_b = \frac{1}{1/(K_{ce})_b + 1/(K_{bc})_b}$$

The coefficient of gas interchanges between the bubble and the cloud wake region based on the volume of the bubbles

$$(K_{bc})_b = 4.5\left(\frac{U_{mf}}{d_b}\right) + 5.85\frac{D_g^{1/2}g^{1/4}}{d_b^{5/4}}$$

The coefficient of gas interchanges between the cloud wake region and the emulsion phase based on the volume of the bubbles

$$(K_{ce})_b = 6.78\left(\frac{\varepsilon_{mf} D_{eff} U_b}{d_b^3 \delta_b}\right)^{1/2}$$

The evaporation coeff can be estimated using

$$\sigma = \frac{h_p \rho_g D_g}{k_g}$$

Heat transfer coefficient between drying gas and solid

$$h_p = c_g U_0 \rho_g j_h \mathrm{Pr}_g^{-2/3}$$

The Colburn factor is given by

$$j_h = \frac{Nu_p}{\mathrm{Re}_p \mathrm{Pr}_g^{1/3}} = \{1.77 \mathrm{Re}_p^{-0.44} \mathrm{Re}_p \geq 30; 570 \mathrm{Re}_p^{0.78} \mathrm{Re}_p < 30$$

The Nusselt number is given by

$$Nu_p = \frac{h_p d_p}{k_g}$$

The Prandlt number is given by

$$\mathrm{Pr}_g = \frac{c_g \mu_g}{k_g}$$

The Reynolds number is given by

$$\mathrm{Re}_p = \frac{d_p U_0 \rho_g}{(1-\varepsilon_{mf})\mu_g}$$

The volumetric coefficient between the bubble and the emulsion phase based on the volume of the bubble

$$(H_{be})_b = \frac{1}{1/(H_{bc})_b + 1/(H_{ce})_b}$$

The volumetric coefficient between the bubble and the cloud wake region based on the volume of the bubble

$$(H_{bc})_b = 4.5\frac{U_{mf} \rho_g c_g}{d_b} + 5.85\frac{(k_g \rho_g c_g)^{1/2}}{d_b^{5/4}} g^{1/4}$$

The volumetric coefficient between the cloud wake region and the emulsion phase based on the volume of the bubble

$$(H_{ce})_b = 6.78(\rho_g c_g k_g)^{1/2}\left(\frac{\varepsilon_{mf} U_b}{d_b^3 \delta_b}\right)^{1/2}$$

The average moisture content of gas bubbles is given as

$$\bar{x}_b = \frac{1}{H_f}\int_0^{H_f} x_b dz$$

SOLUTION OF THE NUMERICAL MODEL

The solution of the model equations is obtained through a two-dimensional trial-and-error procedure. For simplification, first we seek to reduce the integro differential equations to a set of first-order differential equations.

$$X_p^* = \frac{1}{t_s}\int_0^{t_s} x_p^* \exp\left(\frac{-t_s}{\bar{t}_s}\right) dt_s$$

$$\frac{dX_p^*}{dt_s} = \frac{x_p^*}{\bar{t}_s}\exp\left(\frac{-t_s}{\bar{t}_s}\right)$$

Boundary condition

$$X_p^* = 0 \quad \text{at} \quad t_s = 0$$

$$T_p^* = \frac{1}{\bar{t}_s}\int_0^{t_s} T_p \exp\left(\frac{-t_s}{\bar{t}_s}\right) dt_s$$

$$dT_p^* = \frac{T_p}{\bar{t}_s}\exp\left(\frac{-t_s}{\bar{t}_s}\right)$$

Boundary condition

$$T_p^* = 0 \quad \text{at} \quad t_s = 0$$

$$T_b^* = \frac{1}{H_f}\int_0^{z} T_b dz$$

$$\frac{dT_b^*}{dz} = \frac{T_b}{H_f}$$

Boundary condition

$$T_b^* = 0 \quad \text{at} \quad t_s = 0$$

$$\overline{x_p^*} = X_p^* \big|_{t_s = t_s^0} + x_p^* \big|_{t_s = t_s^0} \exp\left(-\frac{t_s^0}{\bar{t}_s}\right)$$

$$T_p = T_p^* \big|_{t_s = t_s^0} + T_p \big|_{t_s = t_s^0} \exp\left(-\frac{t_s^0}{\bar{t}_s}\right)$$

$$\overline{T_b} = T_b^* |_{z=H_f}$$

Now the solution of the governing Eqs. (1), (2), (3), (4), (5) and (6) with the corresponding boundary and initial conditions would be obtained by using the 4th order Runge-Kutte method. Initially data consisting of physical properties, bed dimensions and boundary conditions are entered and the values of unknown parameters such as x_c and T_c are guessed. The calculated values through Eqs. (2) and (5) compared with the initial guess. The program running is finished while the difference between the old and calculated values of x_e and T_e is within the acceptable tolerance.

Our guess is accepted if

$$| x_i^{k+1} - x_i^k | / x_i^k < \varepsilon_x$$

$$| T_i^{k+1} - T_i^k | / T_i^k < \varepsilon_t$$

Where ε_x and ε_t are small numbers about $10^{-2} \sim 10^{-4}$.

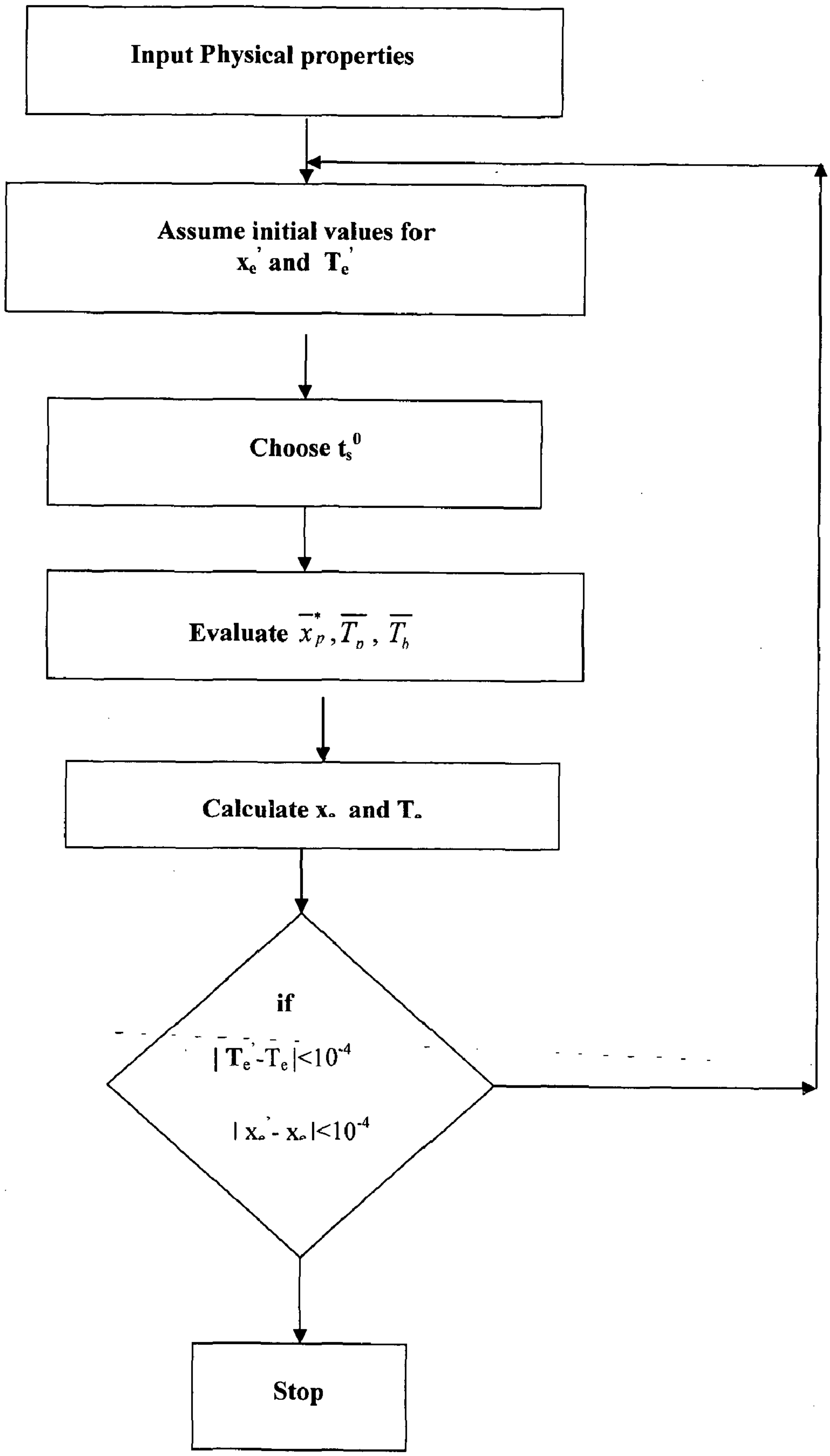

Fig. 4.1 Algorithm of solution

RESULTS AND DISCUSSIONS

A numerical simulation of the fluidized bed dryer based on the two-phase theory of fluidization, which has incorporated a correlation to calculate the bubble diameter has been done.This chapter discusses the results and interpretations of the analysis of a continuous fluidized bed dryer. To validate the numerical solution, the results of the model have been compared with that of Lai and Chen.

5.1 Effect of the operating parameters

The effect of various operating parameter on the characteristics of the dryer performance has been studied. These include the superficial air velocity, temperature of the input solid, residence time of solids in the dryer, particle diameter, initial moisture content of the solid input, density of the solid on the output variables as the moisture content of the output solid and the temperature of the output solid has been studied.

The simulation of fluidized bed dryer based on the two phase theory of fluidization has been done, and the results of the simulation model are found to be in good agreement with that of the data of "Lai and Yiming Chen", with the maximum deviation of 3% fig.5.1. and fig.5.2. shows the interpretation the data.

The horizontal section of the curve fig.5.2. represents the constant-rate drying period with the temperature of the particle equal to the wet-bulb temperature. The corresponding portion of the x_p (t,) curve Fig.5.1. is a linearly declining section. The remaining portion of each of the two curves represents the falling rate drying period in which the temperature and moisture content of the particle approach gradually their respective equilibrium values.

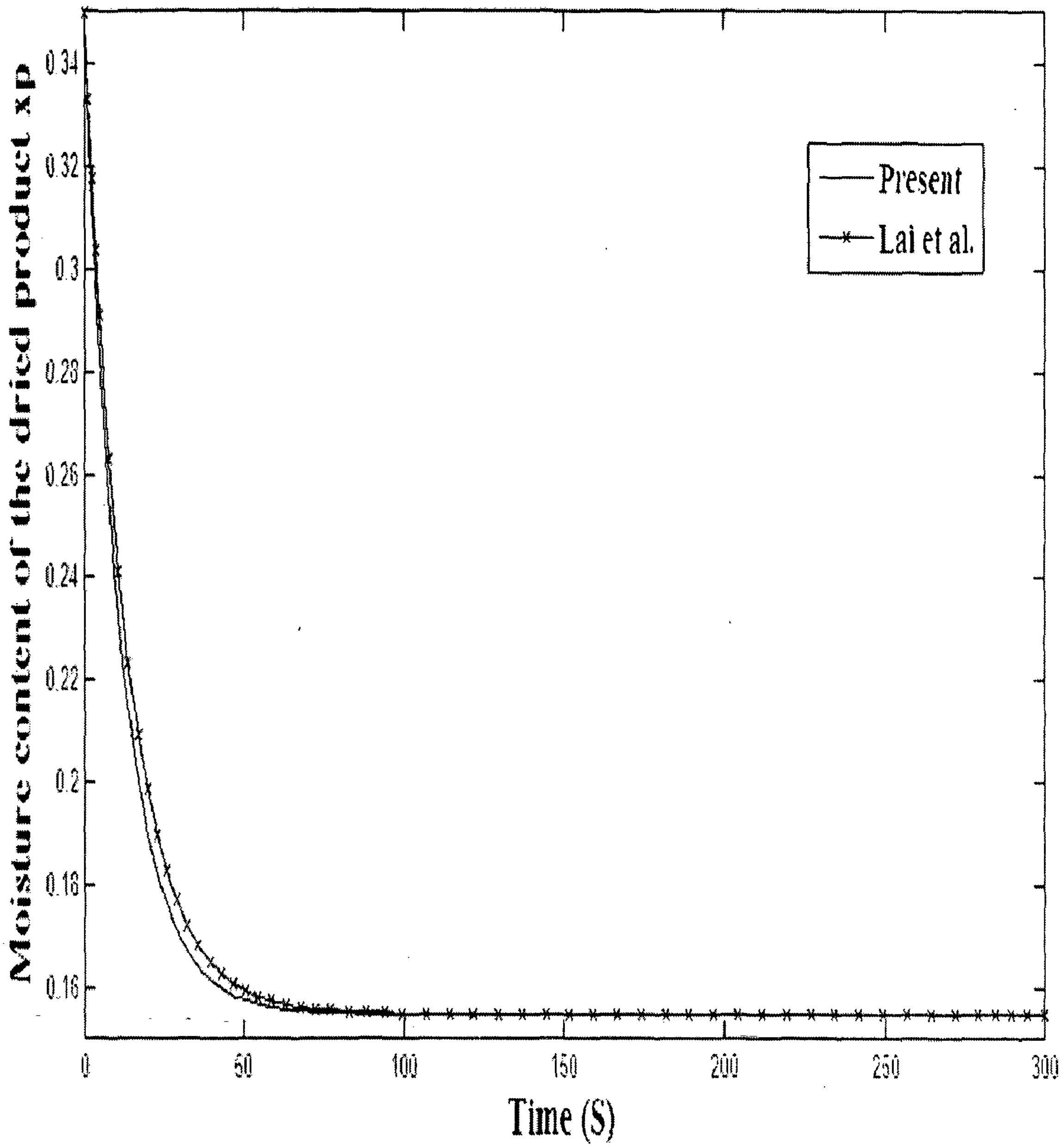

Fig .5.1. Comparison of the moisture content of the outlet solid particle as a function of Time

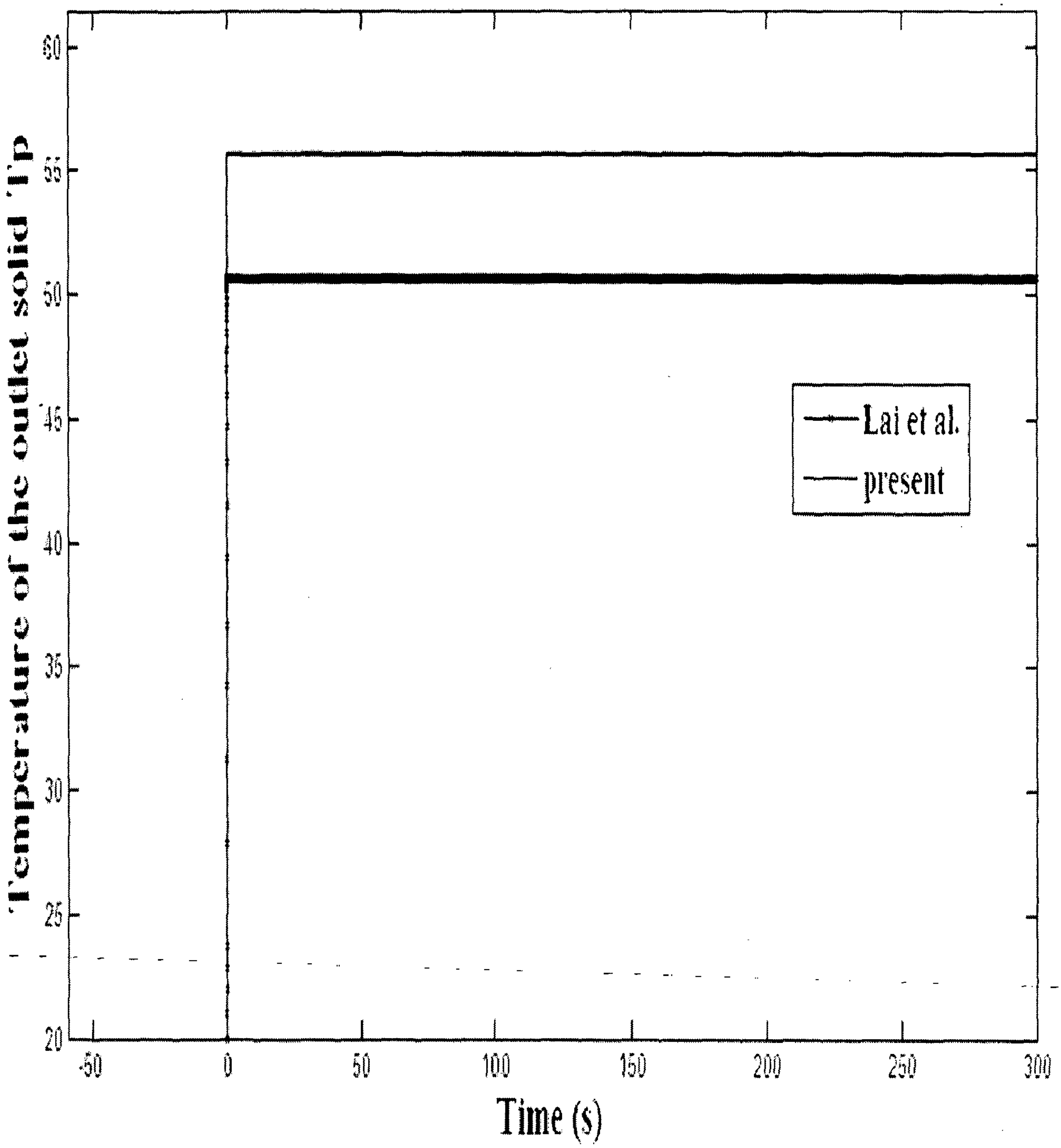

Fig.5.2. Comparison of the temperature of the outlet solid particle as a function of time

Fig.5.3. shows the effect of Moisture content of the inlet solid particle as a function of time on the moisture content of the outlet solid.

From the curves we can observe that by increasing the inlet moisture content of the solid particle decreases the drying rate slightly which in turn increases the residence time of solids in the bed. A possible explanation can be, that the higher inlet gas humidity results higher average moisture concentration in the bubble-phase and also in the interstitial-gas. But this causes decrease in drying rate and indirectly decreasing bubble phase concentration. Because of these counter effects, the resultant change in the drying rate can be small.

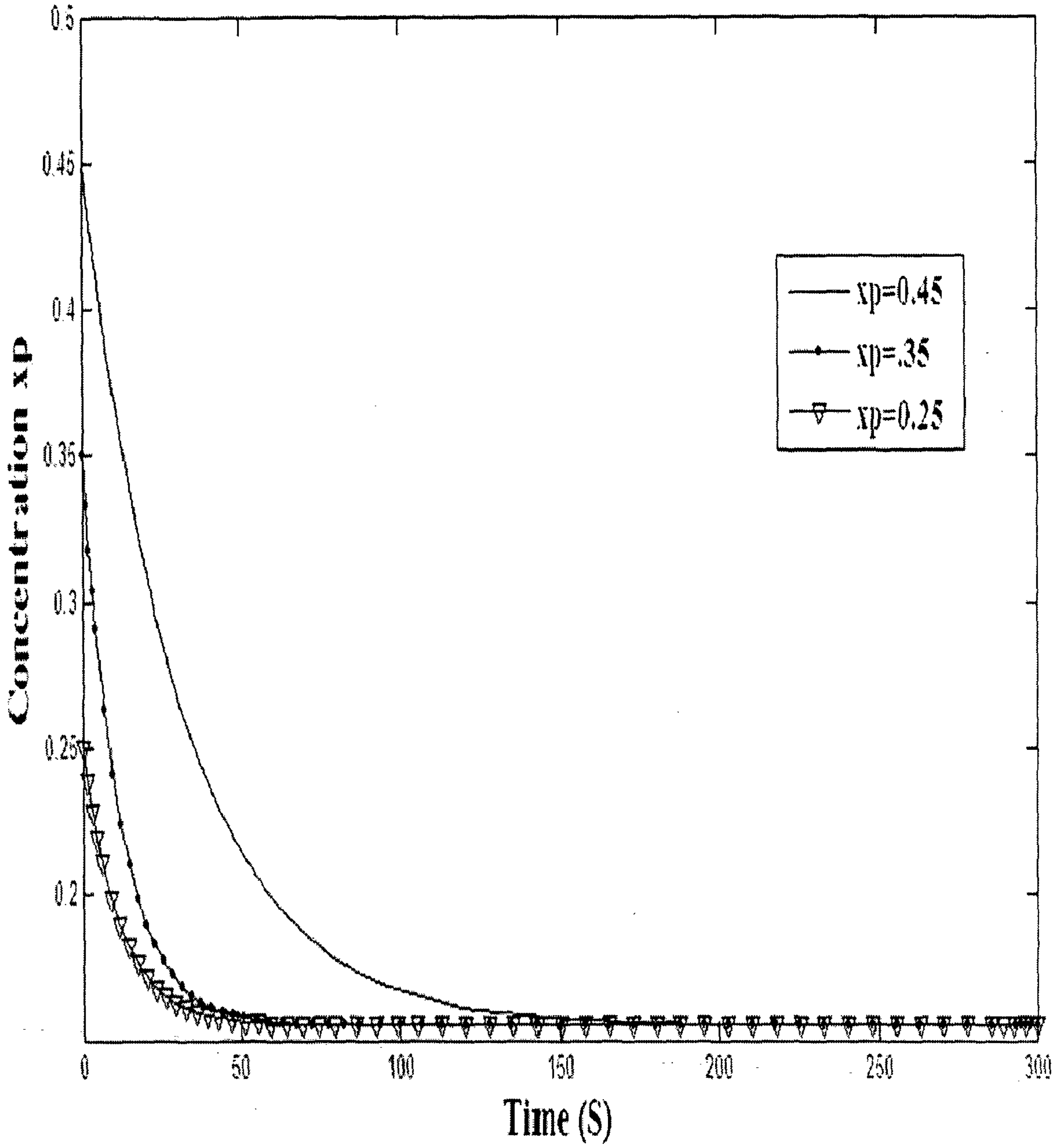

Fig.5.3. Variation of moisture content of the dried product as a function of time and initial moisture content

Fig.5.4. shows the effect moisture content of the dried product as a function of time and superficial air velocity.

The comparison of the results demonstrate that when the superficial air velocity is increased the average temperature of the particles at the exit increases appreciably while their average moisture content reduces sharply. As the superficial air velocity is increased the time taken by the particle to reach equilibrium moisture content has been reduced, and it increases with the decrease in the superficial air velocity.

The higher inlet-gas velocity increases the heat and mass transfer between the bubble-phase and the interstitial gas as well as between the interstitial gas and the solid particles. On the other hand, considering that the gas flow rate in the fluidized bed also grows, the humidity concentration in the interstitial gas may get reduced. These effects can reduce the moisture content of the solid outlet.

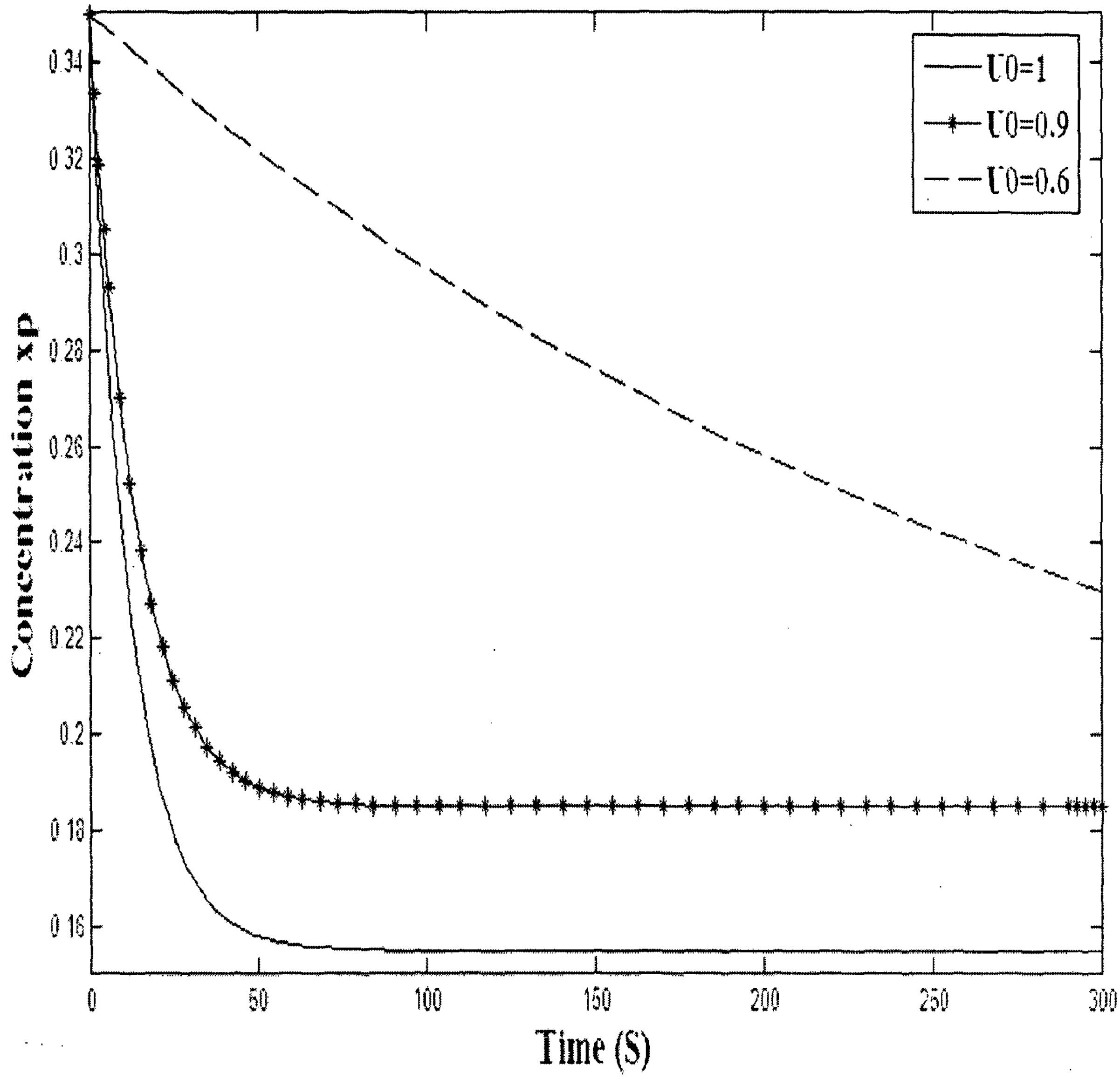

Fig.5.4. Variation of moisture content of the dried product as a function of time and superficial air velocity

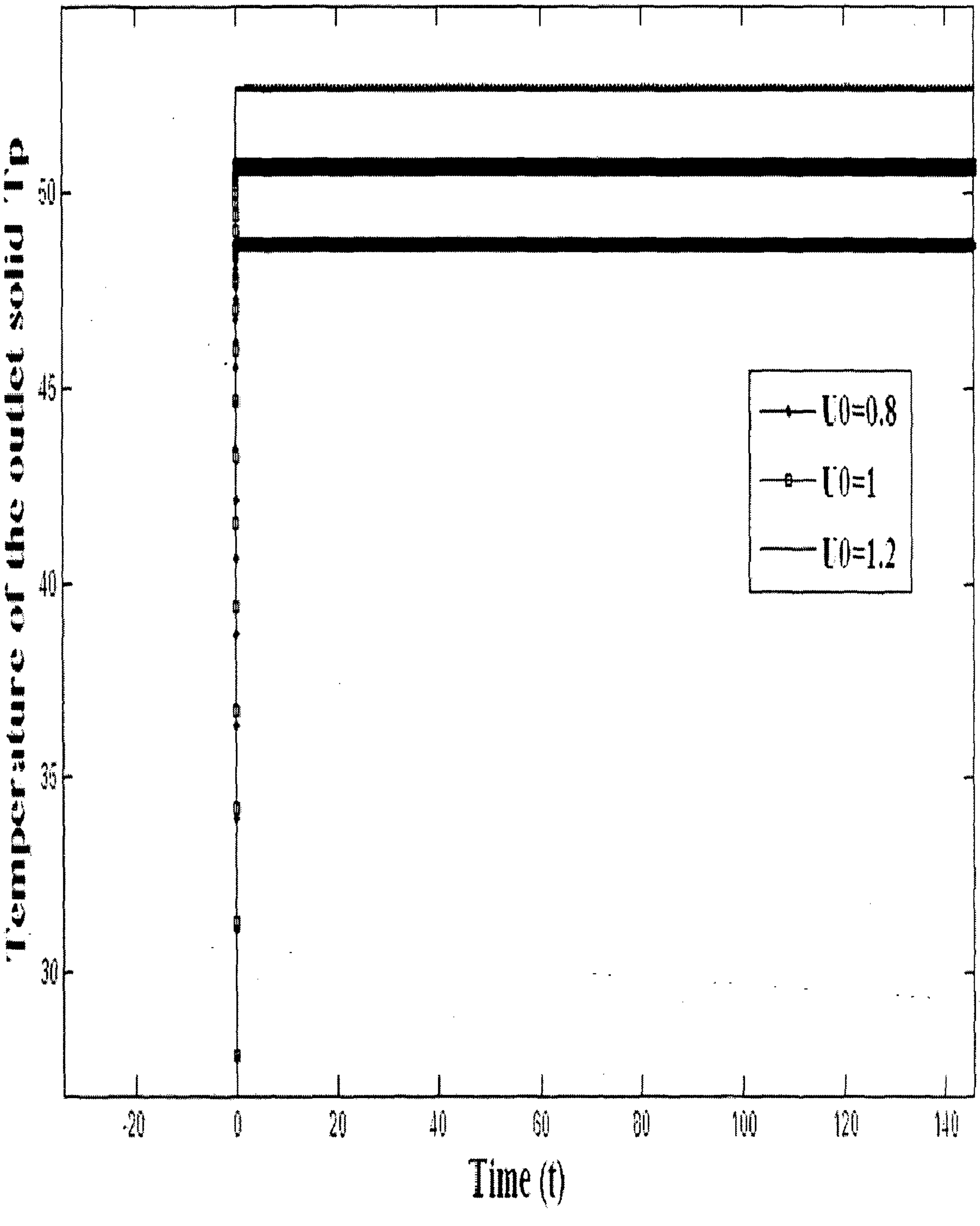

Fig.5.5. Variation in the temperature of the dried product as a function of time and superficial air velocity

Fig.5.6. and fig.5.7 shows the effect moisture content of the dried product as a function of time and mean residence time of the solid particle.

Fig.5.6 and Fig.5.7 discusses the effect of mean residence time of particle on the dryer performance . with the bed height being fixed the smaller the mean residence time, the larger the feed flow rate of solids and the shorter the contact time between the particles and the drying gas, which results in a relatively low average temperature and a high moisture content for the particles at the exit.

The growth of the average residence time of the particles increases the contact-time, effecting longer drying time and thus it lessens the moisture content of the solid outlet.

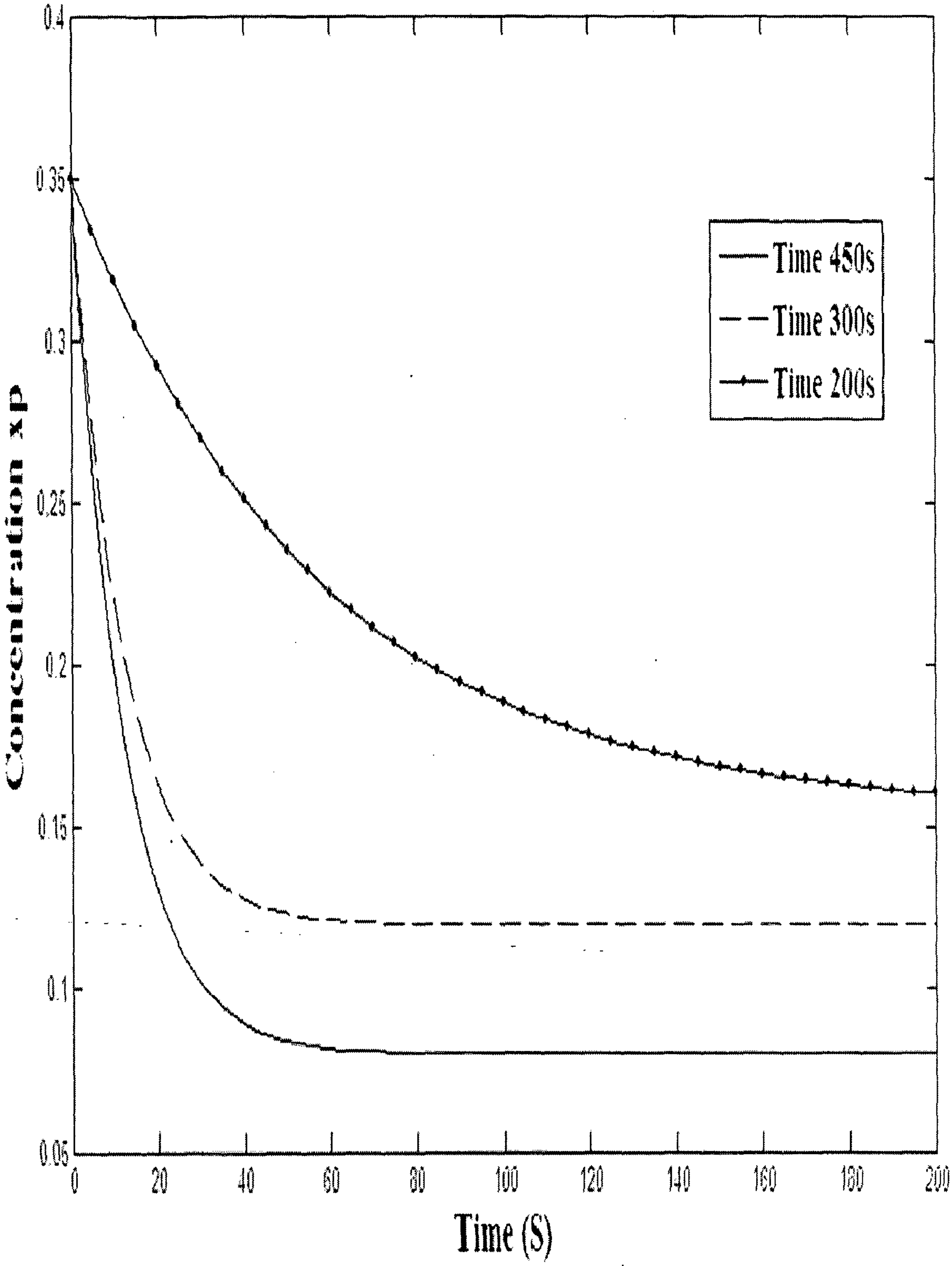

Fig.5.6. Variation of moisture content of the dried product as a function of time and residence time of the solid particle

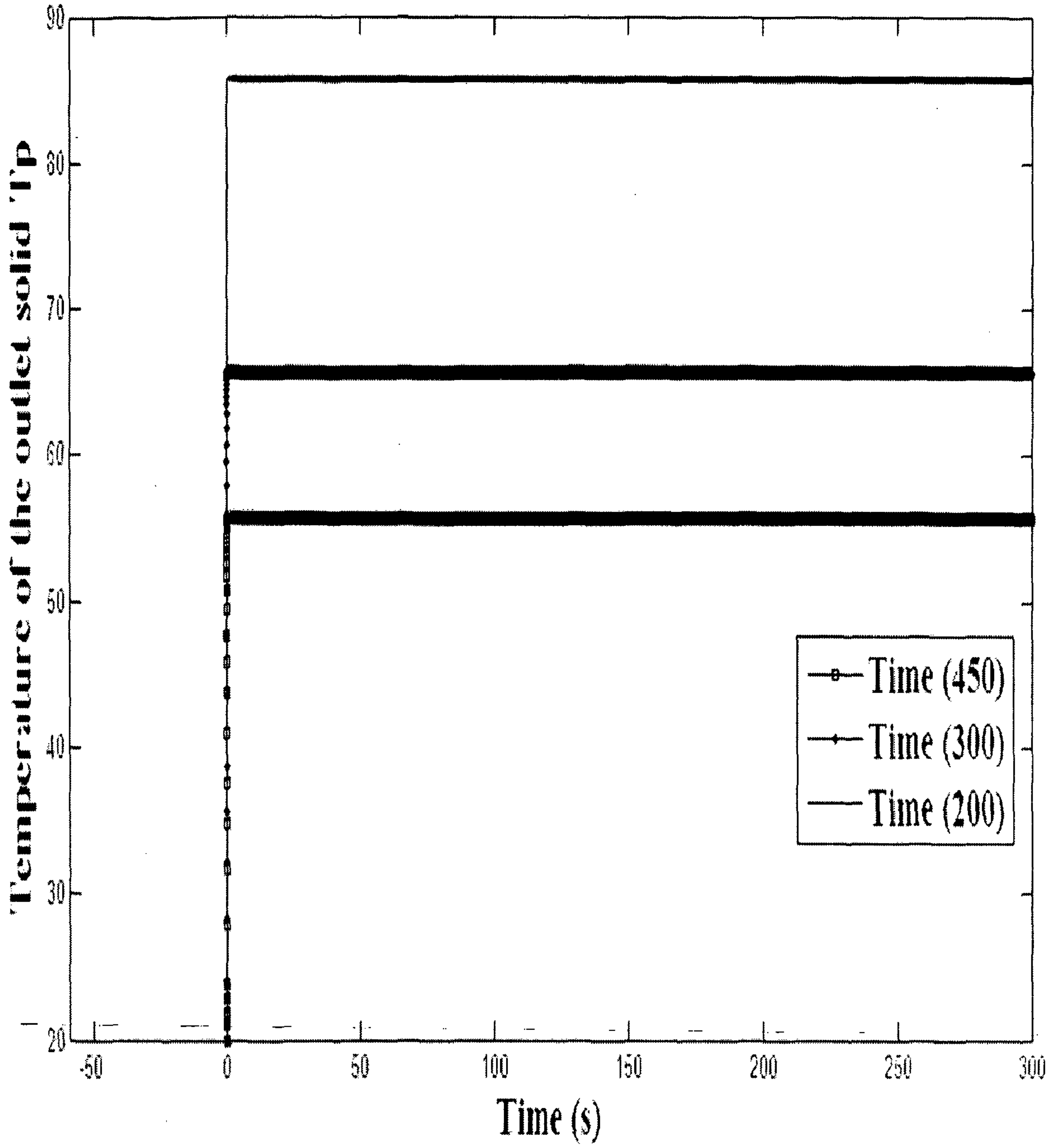

Fig.5.7. Variation in temperature of the dried product as a function of time and residence time of the solid particle

Fig.5.8. shows the effect moisture content of the dried product as a function of time and initial temperature of the solid particle

The comparision of the results demonstrate that the inlet particle temperature has negligible effect on the dryer performance.

Fig.5.9. shows the effect moisture content of the dried product as a function of time and particle diameter.

From the figure it can be seen that a relatively small increase in the particle diameter may result higher outlet moisture content, because the Reynolds number and accordingly the heat and mass transfer between the particles and the interstitial gas decrease.

Fig.5.10. shows the effect moisture content of the dried product as a function of time and particle diameter.

From the figure it can be seen that a slight decrease in the particle density has negilible effect on the outlet moisture content of the solid particle.

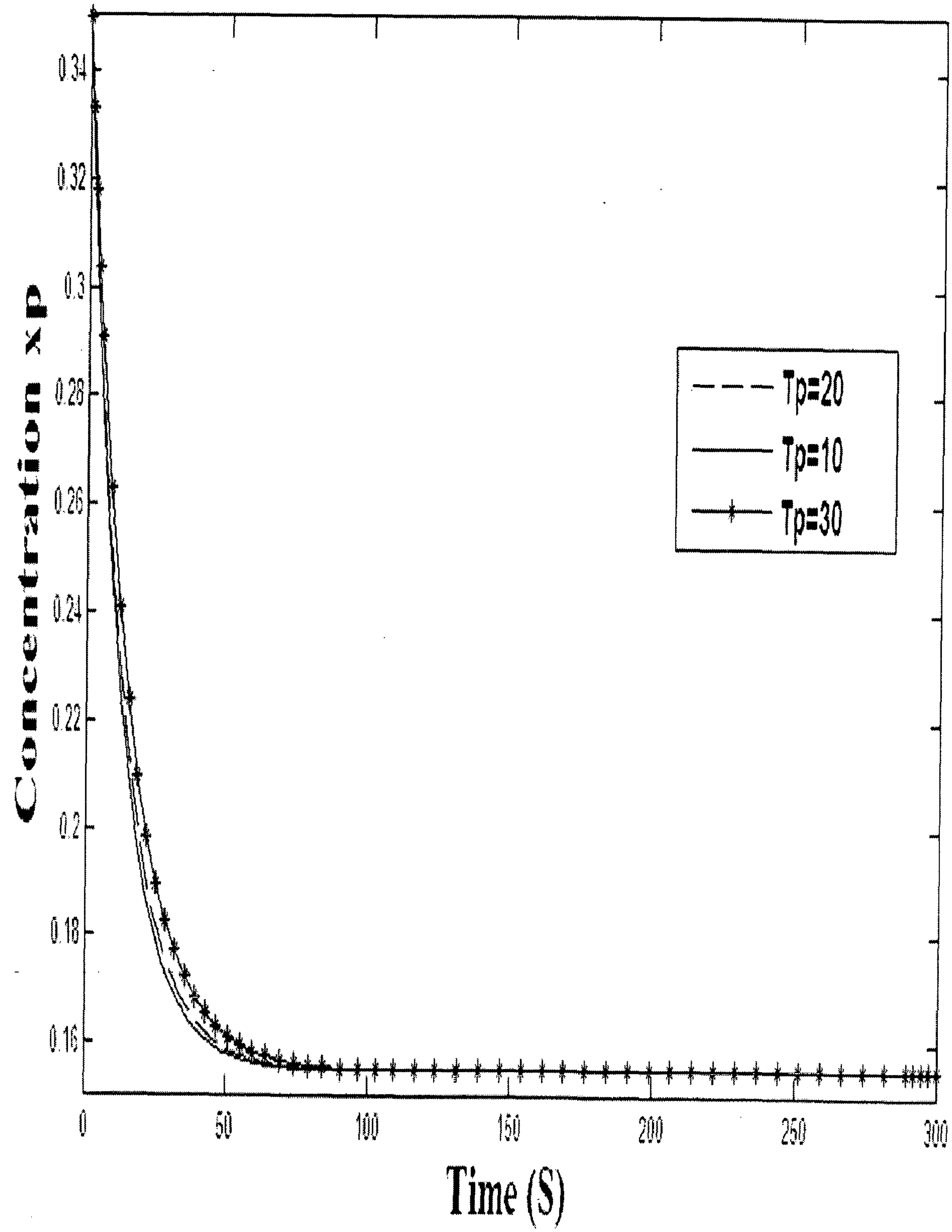

Fig.5.8. Variation in moisture content of the dried product as a function of time and initial temperature of the solid particle

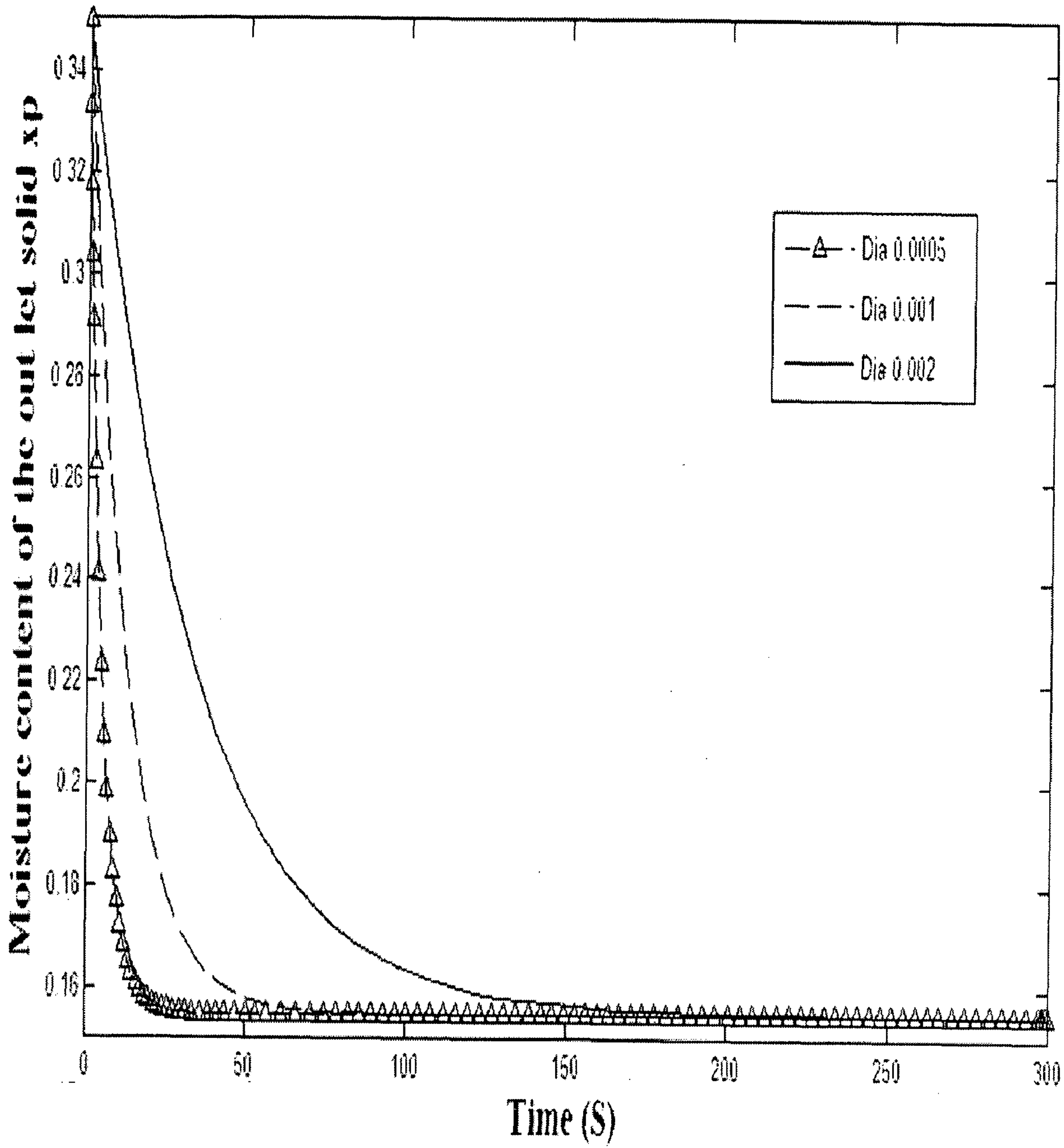

Fig.5.9. Variation of moisture content of the dried product as a function of time and Particle diameter

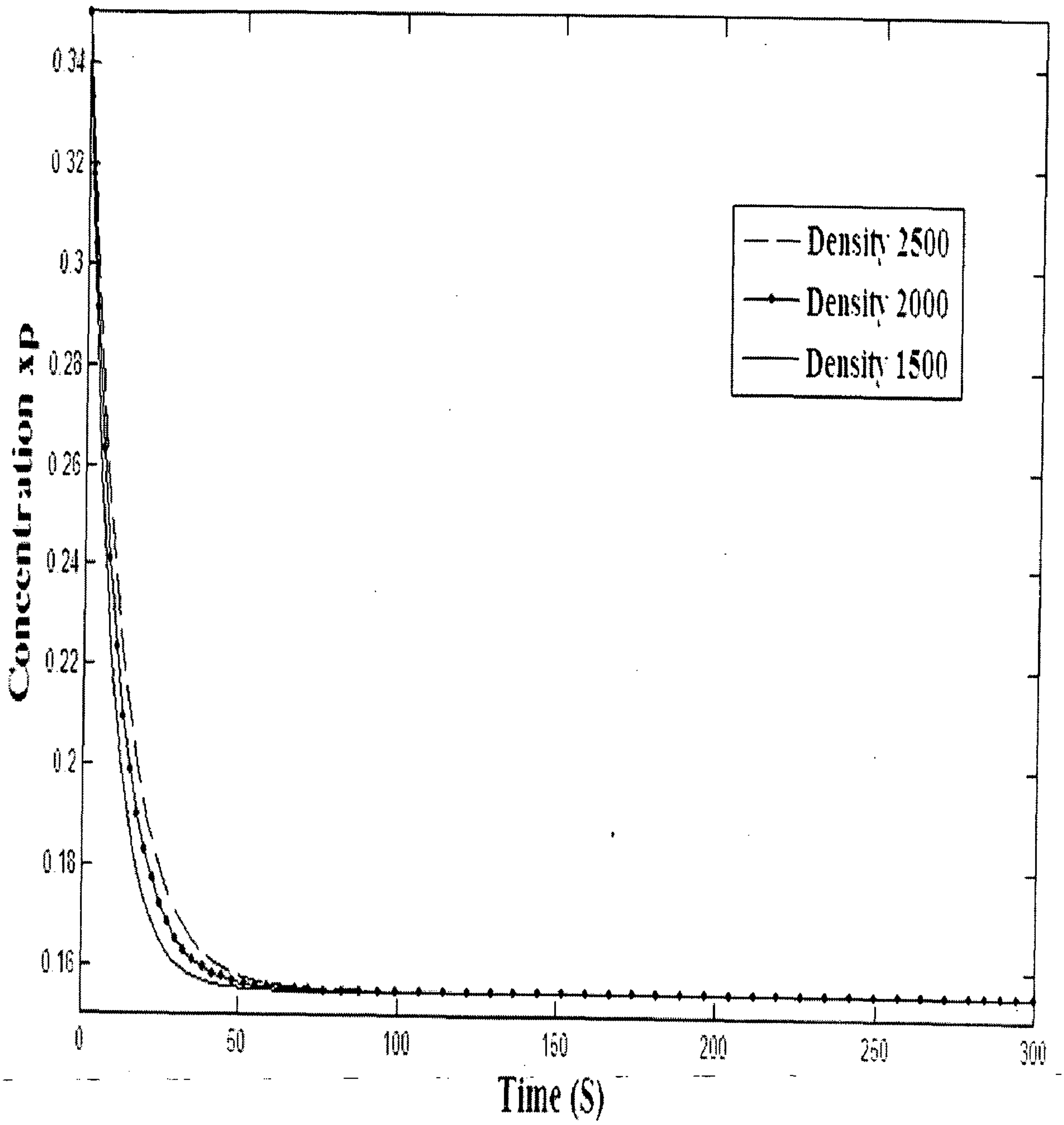

Fig.5.10. Variation of moisture content of the dried product as a function of time and solid density

RECOMMENDATIONS & CONCLUSION

6.1. Conclusion:

A mathematical model for continuous drying in fluidized-bed based on the two phase theory of fluidization was presented. Numerical computation based on this model was carried out and the results of the model are in good agreement with the data of "Lai and Yiming Chen. The current model has incorporated a correlation which was used to calculate the diameter of the bubble. The influence of various operating parameters, such as particle diameter, particle density, superficial gas velocity, inlet solid temperature, residence time and the moisture content of the solid inlet, has been studied. The effect of these parameters on the outlet variables that are solid moisture content and the temperature has been investigated.

In contrast to the previous models, the uniformity of the bubble size along the height of the bed is not assumed. Therefore, the bubble diameter varies along the bed height. While the bubble size increases in the bed, causes reduction in the mass and heat transfer rate, leads to a relative reduction in particle temperature as well as a relative increase in the moisture content of particles.

6.2. Recommendations:

However, to make the model more realistic, it seems to be advisable to improve the lumped particle model and to take the internal resistances to the heat and mass transport inside the moisture solid into account.

These results also indicate that the fluidized-bed dryer is effective in enhancing the drying rate mainly in the constant drying period. Thus, it appears advisable that a fluidized-bed dryer be used in series with a conventional moving-bed or packed-bed dryer the latter serves to dry particles with bound moisture content.

1. Davidson J.F., Clift .R, Harrison .D, "*Fluidization*", second ed., Academic Press, 1985.
2. Leva M., "*Fluidization*", McGraw-Hill, New York 1959.
3. Broadhurst T.E., Becker .H.A., "*Onset of fluidization and slugging in beds of uniform Particles*", AIChE 21 (2) (1975) 238–247.
4. Mori S., Wen C.Y, "*Estimation of bubble diameter in gaseous fluidized beds*", AIChE 21 (1) (1975) 109–115.
5. Grace J.R., "*Effect of bubble interaction on inter phase mass transfer in gas fluidized beds*" Chemical Engineering Science Vol. 36, pp. 327-335 (1981)
6. Palancz .B, "*Mathematical model for continuous fluidized bed drying*", Chemical Engineering Science 38 (7) (1983) 1045–1059.
7. Lai F.S., Chen .Y, "*Modeling and simulation of a continuous fluidized bed dryer*", Chemical Engineering Science 41 (9) (1986) 2419–2430.
8. McCabe, W.L., Smith, J. C., Harriott, P., 1987, "*Unit Operations of Chemical Engineering*", Fourth Edition, McGraw-Hill Book Company, Singapore.
9. Edward J. Boyle "*Modelling of solid particles in fluidized beds*" mathi Comput. Modelling, Vol 14, pp, 785-789, 1990
10. Liedy W., Hilligardt K., "*A Contribution to the Scale-Up of Fluidized Bed Driers and Conversion from Batchwise to Continuous Operation*", Chem. Eng. Process., 30 (1991) 51-58
11. Kunii D., Levenspiel O., "*Fluidization Engineering*", 2nd Edition, Butterworth-Heinemann, Division of Reed publishing, New York, 1991.
12. Geankoplis, C.J., 1993, "*Transport Processes and Unit Operations*", 3 rd Edition, Prentice-Hall International, Inc., New Jersey.
13. Molerus O., Burschka A., Dietz S., "*Particle migration at solid surfaces and heat transfer in bubbling fluidized beds--ii. prediction of heat transfer in bubbling fluidized beds*" Chemical Engineering Science, Vol. 50, No. 5, pp. 879 885, 1995
14. Wiman J., Almstedt A. E., "*Influence of pressure, fluidization velocity and particle size on the hydrodynamics of a freely bubbling fluidized bed*" Chemical Engineering Science, Vol. 53, No. 12, pp. 2167-2176, 1998

15. S. J. Temple & A. J. B. van Boxtel " *Modelling of Fluidized-bed Drying of Black Tea*" J. agric. Engng Res. (1999) 74, 203-212.

16. S. J. Temple1, A. J. B. van Boxtel "*Fluidization of Tea*"J. agric. Engng Res. (1999) 74, 5}11

17. S. J. Temple1 & A. J. B. van Boxtel "*Thin Layer Drying of Black Tea* " J. agric. Engng Res. (1999) 74, 167}176.

18. Zhao Hui Wang., Guohua Chen., "*Heat and mass transfer in batch fluidized-bed drying of porous Particles*" Chemical Engineering Science 55 (2000) 1857-1869

19. Syahrul S., Dincer I., Hamdullahpur F., "*Thermodynamic modeling of fluidized bed drying of moist particles*" International Journal of Thermal Sciences 42 (2003) 691–701

20. Jie Lib., Kuipersa J.A.M., " *Gas-particle interactions in dense gas fluidized beds* " Chemical Engineering Science 58 (2003) 711 – 718

21. Wang X.S., Rhodes M.J., "*Determination of particle residence time at the walls of gas fluidized beds by discrete element method simulation*" Chemical Engineering Science 58 (2003) 387 – 395

22. Patil D.J., van Sint Annaland M., Kuipers J.A.M., "*Critical comparison of hydrodynamic models for gas–solid fluidized beds—Part II: freely bubbling gas–solid fluidized beds*" Chemical Engineering Science 60 (2005) 73 – 84

23. Baker C.G.J., Khan .A.R., Ali Y., Damyar K., "Simulation of plug flow fluidized bed dryers" Chemical Engineering and Processing 45 (2006) 641–651

24. Deen .N.G., Van Sint Annaland M., Van der Hoef M.A., Kuipers J.A.M., "*Review of discrete particle modeling of fluidized beds*" Chemical Engineering Science 62 (2007) 28 – 44

25. Assari M.R., Basirat Tabrizi H., Saffar-Avval M., "*Numerical simulation of fluid bed drying based on two-fluid model and experimental validation*" Applied Thermal Engineering 27 (2007) 422–429

APPENDIX-I

$U_0 = 1 \text{ m s}^{-1}$

$T_0 = 100\ ^0\text{C}$

$x_0 = 0.015$

$\rho_g = 1 \text{ kg m}^{-3}$

$\gamma_0 = 2.5 \text{ X } 10^3 \text{ KJ kg}^{-1}$

$\mu_g = 2 \text{ X } 10^{-5} \text{ kgm}^{-1} \text{ s}^{-1}$

$\rho_s = 2500 \text{ kg m}^{-3}$

$\rho_w = 1000 \text{ kg m}^{-3}$

$\phi = 1$

$x_{p0} = 0.35$

$x_{pc} = 0.2$

$c_g = 1.06 \text{ kJ kg}^{-1}\ ^0\text{C}^{-1}$

$c_p = 1.26 \text{ kJkg}^{-1}\ ^0\text{C}^{-1}$

$c_w = 4.19 \text{ kJkg}^{-1}\ ^0\text{C}^{-1}$

c_{wv} = 1.93 kJkg-1 0C-1

$D_c = 0.15 \text{ m}$

$D_g = 2 \text{ X } 10^{-5} \text{ m}^2 \text{ s}^{-1}$

$d_p = 0.001 \text{ m}$

$g = 9.8 \text{ m s}^{-2}$

$H_f = 0.5 \text{ m}$

$k_g = 2.93 \text{ X}10^{-2} \text{ Jm}^{-1}\ ^0\text{C}^{-1}$